

Review

# Coatings for Automotive Gray Cast Iron Brake Discs: A Review

Omkar Aranke <sup>1,\*</sup> , Wael Algenaid <sup>1,\*</sup> , Samuel Awe <sup>2</sup>  and Shrikant Joshi <sup>1</sup> <sup>1</sup> Department of Engineering Science, University West, 46132 Trollhättan, Sweden<sup>2</sup> R & D Department, Automotive Components Floby AB, 52151 Floby, Sweden

\* Correspondence: omkar.aranke@outlook.com (O.A.); wael.alfatih@outlook.com (W.A.)

Received: 7 August 2019; Accepted: 23 August 2019; Published: 27 August 2019



**Abstract:** Gray cast iron (GCI) is a popular automotive brake disc material by virtue of its high melting point as well as excellent heat storage and damping capability. GCI is also attractive because of its good castability and machinability, combined with its cost-effectiveness. Although several lightweight alloys have been explored as alternatives in an attempt to achieve weight reduction, their widespread use has been limited by low melting point and high inherent costs. Therefore, GCI is still the preferred material for brake discs due to its robust performance. However, poor corrosion resistance and excessive wear of brake disc material during service continue to be areas of concern, with the latter leading to brake emissions in the form of dust and particulate matter that have adverse effects on human health. With the exhaust emission norms becoming increasingly stringent, it is important to address the problem of brake disc wear without compromising the braking performance of the material. Surface treatment of GCI brake discs in the form of a suitable coating represents a promising solution to this problem. This paper reviews the different coating technologies and materials that have been traditionally used and examines the prospects of some emergent thermal spray technologies, along with the industrial implications of adopting them for brake disc applications.

**Keywords:** gray cast iron; brake discs; automotive; emissions; coatings; thermal spray; high velocity air fuel (HVOF); suspension plasma spraying (SPS)

## 1. Introduction

Brake discs, also known as brake rotors, are a crucial part of the automotive braking system which slows down the vehicle by converting kinetic energy into thermal energy, and consequently increases the temperature of the disc friction surfaces. Brake discs have a larger sweep area and higher exposure to air flow than the traditionally used drum brakes and, therefore, cool down at a fast rate [1]. Gray cast iron (GCI) is the most commonly used brake disc material due to its high damping capability and desirable thermophysical properties (melting point, thermal conductivity, and heat storage capacity) which prevents overheating, brake noise, and brake fade [1–4]. However, the poor corrosion resistance of GCI leading to brake judder [5,6], high weight contributing to increased fuel consumption [7], and brake wear emissions in the form of brake dust and particulate matter [8–10] are some of the major disadvantages of GCI.

Over the past decade, several alternative materials such as metal matrix composites (MMC), ceramic matrix composites (CMC), and titanium alloys have also been proposed and tested for automotive brake disc applications, with light-weighting being the primary motivation. Table 1 enlists the main mechanical and thermal properties of some of these materials. The most notable advantage of GCI over other materials is its combination of high melting point and thermal conductivity, which provides excellent thermal stability, apart from cost-effectiveness.

Among these materials, aluminum MMCs have demonstrated good resistance to corrosion and wear whilst offering significant reduction in weight [3,11]. However, it has issues such as lower melting temperature and higher coefficient of thermal expansion as compared to GCI [12–14]. Lightweight titanium alloys have demonstrated 37% reduction in weight as compared to cast iron but their wear rate has been found to be higher than GCI [15]. Carbon–carbon composites represent yet another class of materials that has been used predominantly for aircraft and motor racing applications, but their inherently high cost and poor braking performance at low temperatures limits their application area [16]. Although not included in Table 1, CMCs such as carbon-fiber reinforced silicon carbide (C/SiC) composites are known to possess excellent thermal stability up to 1300 °C, superior tribological properties over GCI along with significant weight savings but suffer from very high costs and are consequently notably used only in high performance racing cars and luxury vehicles [17–19].

**Table 1.** Mechanical and thermal properties of promising brake disc materials at room temperature.

Material	Melting Point (°C)	Bulk Density (g/cm <sup>3</sup> )	Thermal Conductivity (W/m.K(°C))	Thermal Expansion Coefficient (μstrain/°C)	Vickers Hardness (HV)	Youngs Modulus (GPa)	Poisson's Ratio
GCI	1200	7.2	50–72	11–13	90–216	80–100	0.27
Al-12SiC	630	2.8	120–130	17.7–18	91–138	94–98	0.3
Ti 6Al-4V	1600	4.43	8–9	8.7–9.1	332–336	113–115	0.34
Carbon-carbon composite	3300	1.7	13–35	1.1–8.4	42–46	71–79	0.32

Data reported in Table 1 has been extracted from [20].

Apart from the drawbacks associated with alternative lightweight materials, the environmental and health concerns due to production of fine particles during braking of composite brake discs can be a concern and have not yet been addressed completely [21]. Thus, one of the key factors in developing new, light weight, wear and corrosion resistant disc brake materials will also be the need to optimize the characteristics of the associated tribo-surfaces. On account of the above stated drawbacks of the alternate materials and the concomitant need to develop a suitable friction pad material which can be used with these alternative materials, GCI will continue to be the material of choice for brake discs in the near future, especially for passenger vehicles [22].

Notwithstanding the above, problems associated with wear and corrosion of GCI brake discs also need to be urgently addressed since the adverse effects on health due to emission of dust and particulate matter in the atmosphere are already well known [23–25]. According to recent investigations, brake wear generates up to 55% by mass of non-exhaust emissions ensuing from automobiles. Of specific concern is the fact that approximately 50% of the particles generated from brake wear become airborne, with 80%–98% of them being in the PM10 (particulate matter having diameter of 10 μm or less) range [26–28]. The limits on these emissions set by the European Commission (EC) and by the Environmental Protection Agency (EPA) are certain to become stricter in the foreseeable future, which will force automotive industries to search for techno-economically viable solutions [29]. One promising approach is to seek appropriate surface treatment solutions which can reduce the wear and corrosion of GCI brake discs while maintaining or enhancing their functional performance. In anticipation of more stringent environmental regulations being inevitable, the coatings' approach to mitigate disc wear has been considered by a growing number of research groups in recent times. This article considers all the coating technologies which have been already applied on brake discs so far or explored for these applications, as well as some new technologies which can be potentially very promising to comprehensively evaluate.

Notwithstanding their attractive performance, the growing concern with hard chrome is that the plating bath contains hexavalent chromium Cr(VI), which forms a toxic mist during operation and is known to be carcinogenic [30,31]. In the US, the permissible exposure limit (PEL) for hex chrome and its

compounds set by the Occupational Safety and Health Administration (OSHA) is  $5 \mu\text{g}/\text{m}^3$  [32], whereas in Sweden, the limit is set at  $20 \mu\text{g}/\text{m}^3$  [33]. In the automotive industry, the European Parliament and the Council on end-of-life vehicles has set this limit to  $0.025 \text{ mg}/\text{m}^3$  in the EU and the permissible amount is limited to 2 g per vehicle [34]. Such restrictive environmental laws will increasingly limit the use of this technology on a commercial scale and motivate development of other techno-economically viable alternatives.

## 2. Coating Technologies for Brake Discs

Over the years, several different types of coatings have been explored to combat problems of wear and corrosion and some of these have also been considered for automotive brake disc applications. Both, conversion and overlay coatings deposited using various techniques have been suitably applied on automotive components. A brief discussion of the coating techniques which have already been extensively investigated for brake-disc applications is provided below. Since thermally sprayed coatings will be the focus in this article, the techniques are grouped into two broad categories, namely (i) non-thermal spray processes and (ii) thermal spray processes. As subsequently discussed, thermal spray processes concern coating technologies in which feedstock powder particles fed into a high-temperature, high velocity ‘flame’ are heated to a molten/semi-molten state and accelerated before impacting onto a surface to form a coating. The complementary non-thermal spray processes discussed herein mainly comprise electrochemical surface treatment techniques as well as other powder-derived coating processes that complement thermal spray. Furthermore, for the sake of brevity, the following sections are oriented towards and limited to brake disc relevant discussions only.

### 2.1. Non-Thermal Spray Processes

#### 2.1.1. Hard Chrome Plating

It is a traditionally used technology since the 1920s for diverse automotive applications, such as engine valves, brake discs, brake pads, shock absorber rods etc., due to its high hardness, excellent wear and corrosion resistance, low coefficient of friction (CoF), as well as aesthetics [35,36]. Chrome plated coatings having a dense microstructure with very low oxide inclusions have shown excellent resistance to corrosion in harsh environments [37] and very high fracture toughness [30]. The wear resistance of chrome plated coatings has also proven to be superior both in sliding and erosive wear conditions [30,38]. In the study carried out by Balamurugan et al. [39], the chrome plated stainless-steel disc exhibited superior wear resistance, both at low and high temperature, and slightly lower mass loss as compared to the plasma sprayed WC-12Co stainless-steel disc. Similarly, the superior wear resistance of the chrome plated cast iron disc was also reported by Lal et al. [40]. The chrome plated cast iron disc also exhibited a lower CoF as compared to the bare cast iron disc. On the other hand, Krelling et al. [41] found that hard chrome plating on a steel disc had the presence of numerous cracks and microcracks as shown in Figure 1. They reported that the high hardness of the chromium layer resulted in a severe wear of the coating during its pin-on-disc test against an Alumina counter body due to the formation of brittle phases, which was further assisted by these cracks in the coating.

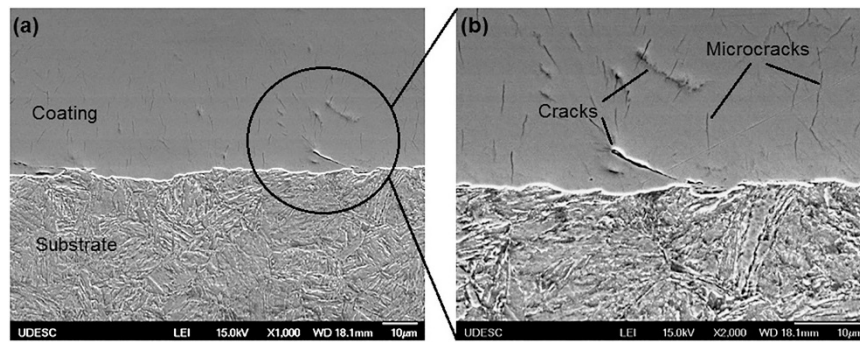


**Figure 1.** Cross sectional micrograph of hard chrome coated specimen showing; (a) coating overview; and (b) detail of the black circle shown in (a) [41]. Reprinted with permission from [41]. © 2018 SciELO.

### 2.1.2. Plasma Electrolytic Oxidation (PEO)

Plasma electrolytic oxidation (PEO) also known as micro-arc oxidation, is an electrochemical surface treatment process for generating oxide coatings on metals and alloys of aluminum, magnesium, titanium, and their composites [42]. The process is similar to anodizing but employs higher voltage and current which results in the discharges creating a plasma on the metal surface [42]. This results in chemical conversion of the metal into its oxide which can grow up to 100 µm in thickness. The coating fabricated by this process is uniform and can be applied on parts with complex geometries [43]. The process does not pose any risk to human health [43] and has been widely developed for many applications including wear resistance [44,45], corrosion protection [45,46], and thermal protection [47].

Alnaqi et al. compared the thermal performance [48] and frictional properties [49] of PEO coated Al-alloy (6082-T6) and Al-MMC (AMC640XA) with GCI brake discs. Both the coatings exhibited higher hardness and stable CoF, although the coating on Al-alloy was more uniform and denser than the coating on Al-MMC. The coated Al-alloy disc showed very good structural integrity at elevated temperatures, although not as good as the reference GCI brake disc. Figure 2 shows the average CoF for the three discs during their dynamometer testing at surface temperature below 200 °C. It can be seen that the CoF of the coated discs is slightly less but still comparable to the GCI brake disc.

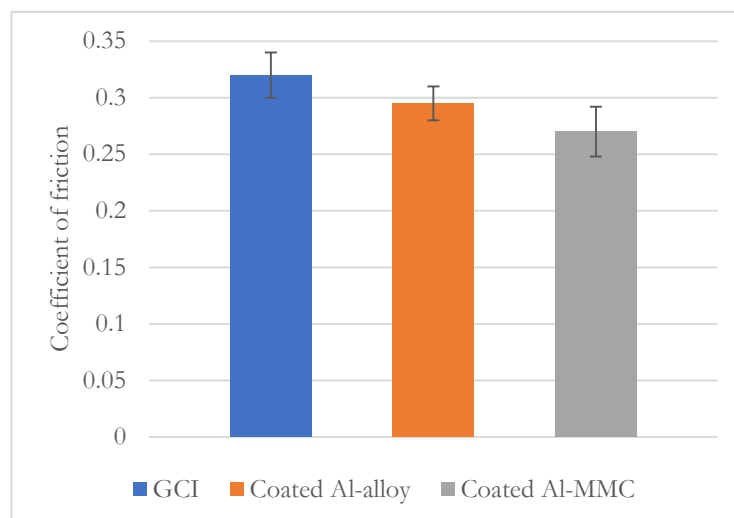


**Figure 2.** Average CoF for 3 different brake disc materials, adopted from Alnaqi et al. [49].

Although PEO coatings have been used widely, the inherent porosity content can be a major drawback. Curran et al. [43] found that the porosity in PEO coatings can reach up to 20% if not controlled properly. Tsai et al. [50] reported that the operation requires high energy and is not often employed for large workpieces due to its high power consumption which can increase operational

costs. It should also be emphasized that the PEO process is only suited for materials like Al-based, Mg-based, and Ti-based composites and their alloys, which form a corresponding protective oxide scale as a conversion coating [51,52]. Therefore, it is inappropriate for GCI brake disc applications, unless application of a prior coating of one of the above metals/alloys can be considered before being subsequently subjected to the PEO process in the form of a duplex coating [53,54].

### 2.1.3. Laser Cladding

Surface treatment by laser cladding is a method that has been increasingly exploited in recent times for various applications to improve wear [55–59] and corrosion resistance [60,61]. This process enables deposition of pore- and crack-free coatings up to 2 mm in thickness with a strong substrate-coating metallurgical bonding and minimal heat input into the substrate [55,56,62,63]. However, some drawbacks with laser cladding on GCI have been reported. De Hosson et al. [62] studied the wear resistance of Co-based coatings deposited on GCI using high power laser cladding. The authors observed cracking inside the coating because of internal stresses gradually built up during the cladding process. Similar cracking was also seen in the study carried out by Fernández et al. [64] in which cracks due to residual stresses were observed in a laser clad NiCrBSi alloy coating, as shown in Figure 3. Sun et al. [65] have also investigated the friction and wear behavior of different materials deposited by laser cladding on compacted GCI substrates and reported a variation in microstructure, composition as well as hardness through the thickness of the coating. Nowotny et al. [58] and Van Acker et al. [55] investigated the maximum volume content of Co and Ni, respectively, in WC-Co and WC-Ni composites deposited by laser cladding. The authors concluded that the maximum volume content for Co is 35% and for Ni is 45% in the composite, as higher values were found to result in large pores, cracks and poor bonding [55,58]. Recently, Zhou et al. [57] found that excessive heat input during laser cladding can lead to decarburization of WC to  $W_2C$  resulting in porosity and crack formation. Due to the above stated limitations, along with the fact that laser clad coatings are easily susceptible to cracking due to the mismatch in the coefficient of thermal expansion between the substrate and coating material, use of this process for brake disc applications has been restricted.

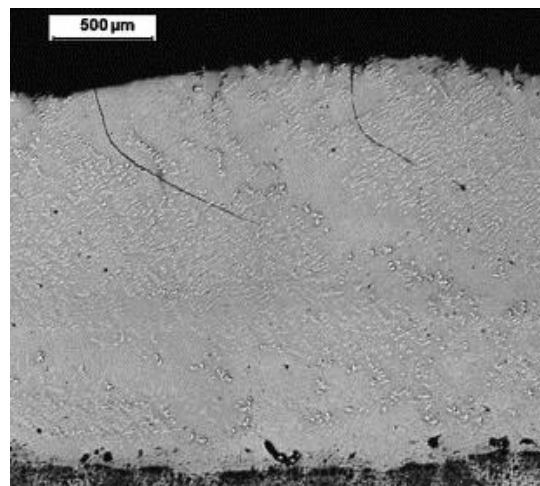


**Figure 3.** Cross sectional micrograph showing cracks in a laser clad NiCrBSi layer [64]. Reprinted with permission from [64]. © 2005 Elsevier.

### 2.1.4. Plasma Transferred Arc (PTA)

As in the case of laser cladding, this process too produces metallurgical bonding between the coating and the substrate, and is capable of depositing thick coatings with high deposition rate in a single layer [66]. Among all the above mentioned surface engineering technologies, PTA also has the additional advantages of high plasma temperature (up to 30,000 °C) to enable complete melting



of feedstock powder, excellent arc stability along with low thermal dilution, and low environmental impact (low oxides emissions) [67,68]. In recent years, PTA has attracted more and more attention for use in sectors such as aircraft, mining, nuclear, and automotive for the purpose of wear and corrosion resistance [69]. Among the wide range of metal powders suited for PTA deposition, Ni- and Co-based alloys are commonly used for high wear- and corrosion-resistant coatings [67]. Apart from the aforementioned advantages, PTA has some problems when used on GCI substrates. Fernandes et al. [70] investigated the factors affecting wear performance of a Ni-based coating deposited on GCI. This study found that dilution from GCI can reach as high as 59% with increasing arc current as shown in Figure 4 and is accompanied by a decrease in hardness as well as wear resistance.

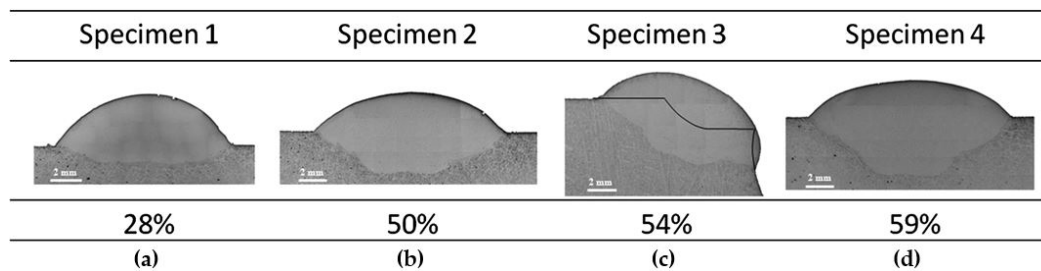


**Figure 4.** A PTA coating showing increase in dilution by GCI from (a) 28%; (b) 50%; (c) 54%; and (d) 59% with increase in arc intensity [70]. Reprinted with permission from [70]. © 2011 Elsevier.

For completeness, the salient features of all the above-mentioned non-thermal spray processes are summarized in Table 2.

**Table 2.** Summary of non-thermal spray processes as candidates for brake disc coating applications.

Coating Process	Source	Possible Coatings	Microstructural Features	References	Drawbacks
Hard chrome plating	Electrolyte	CrO <sub>3</sub>	Metallurgical bonding, highly dense and thin coating	[35,36]	Hexavalent Chromium—carcinogenic
PEO	Electrolyte	Oxides of Al, Mg, Ti	Protective oxide scale, metallurgical bonding and uniform coating thickness	[48,49,71]	Suited only for few metals like Al, Mg, Ti, and their alloys capable of forming protective oxides by chemical conversion
Laser Cladding	Wire or powder	Wide range of Metals alloys, cermets and ceramics	Metallurgical bonding, dense and thick coatings	[57,62,65,72,73]	Different laser beam absorptivity at GCI surface can result in non-homogeneous thermal fields; excessive heating can lead to thermal damage to feedstock (e.g., decarburization of WC to W <sub>2</sub> C)
PTA	Wire or powder	Wide range of Metals, alloys, cermets and ceramics	Metallurgical bonding, dense and thick coatings	[66,70,74,75]	Possibility of dilution from cast iron, to change coating composition and influence mechanical properties

## 2.2. Thermal Spray Processes

Thermal spray is a generic term for a technology that involves a group of coating processes capable of depositing diverse metallic, intermetallic, or ceramic layers on component surfaces for varied functional applications, most often as protection against aggressive environments. In its most common form, the technique relies on injection of powder of the material to be coated into a high-temperature, high-velocity zone where the powder particles are fully/partially molten and propelled at a high particle velocity onto the substrate surface to form a splat. These splats serve as building blocks for forming a coating which is mechanically bonded to the substrate [76]. Different variants of the

thermal spray family are distinguished by the manner in which the high-temperature, high-velocity zone is created and, in turn, are characterized by vastly varying properties. Excellent reviews on different thermal spray techniques, describing the mechanisms of coating formation and the typical features of the resulting coatings are available [77–79]. By virtue of its versatility, thermal spraying is already in commercial use for a wide range of applications spanning aerospace, oil and gas, biomedical, and automotive industries.

The relatively older thermal spray processes such as atmospheric plasma spray (APS) and high velocity oxy-fuel (HVOF) have already been deployed on various automotive engine, suspension and steering, as well as transmission parts [80–82]. Over the years, several APS and HVOF coatings have been considered for automotive brake disc applications to increase the wear and corrosion resistance of the disc material [81,83]. The relatively new thermal spray variants of high velocity air fuel (HVOF) spraying and suspension plasma spraying (SPS) have also been gaining rapid attention due to the advantages over the conventional HVOF and APS technologies, respectively [84,85]. The above technologies have been individually discussed in the subsequent sections, specifically with respect to their relevance for brake disc applications.

### 2.2.1. Atmospheric Plasma Spray (APS)

APS is a widely used commercial process for depositing coatings for numerous functional applications. The typical particle size of feedstock powder ranges from 10 to 100  $\mu\text{m}$ , resulting in splats having diameter ranging from a few tens to hundreds of micrometers [77,86]. The rampant industrial utilization of APS can be linked to its capability to spray a variety of metallic, cermet, or ceramic materials owing to the high temperature of the plasma jet which may exceed 20,000  $^{\circ}\text{C}$  [79,86]. APS coatings have already been in use in the automotive industry to improve the friction and wear properties of piston rings, cylinder blocks, and various other passenger vehicle parts [83,87–90].

Despite its vast potential and widespread industrial acceptance, there are only a few notable works on APS coated brake rotor. Watremez et al. [91] compared the friction coefficient of different ceramic-based coatings, i.e.,  $\text{ZrO}_2$ , yttrium-stabilized zirconia (YSZ) and  $\text{Cr}_3\text{C}_2\text{-}25\text{NiCr}$ , deposited by APS on 4130 steel brake discs. The frictional characteristic of different coated disks against iron copper pads showed that  $\text{ZrO}_2$  and YSZ coatings exhibited higher friction coefficients than an uncoated brake disc ( $\sim 0.65$ ,  $\sim 0.55$  and  $\sim 0.45$ , respectively) at speeds up to 1000 rpm. On the other hand,  $\text{Cr}_3\text{C}_2\text{-}25\text{NiCr}$  coating offered the lowest friction coefficient of  $\sim 0.35$ . Demir et al. [92] compared the frictional performance of GCI brake rotors with GCI rotors having an APS  $\text{Al}_2\text{O}_3\text{-TiO}_2$  coating and an HVOF  $\text{Cr}_3\text{C}_2\text{-NiCr}$  coating. The  $\text{Al}_2\text{O}_3\text{-TiO}_2$  coated brake disc showed negligible weight loss and operated without brake fade at 700  $^{\circ}\text{C}$  after conducting a dynamometer test whereas the bare GCI disc and the  $\text{Cr}_3\text{C}_2\text{-NiCr}$  coated disc had a weight loss of 2 and 4 g, respectively. On similarly coated brake discs, Samur et al. [93] performed sliding wear tests in a salt solution against a 10 mm diameter  $\text{Al}_2\text{O}_3$  counter-ball. Both the coated discs showed lower wear rate of  $1.52 \times 10^{-5}$  and  $1.33 \times 10^{-5} \text{ mm}^3/\text{Nm}$  for  $\text{Al}_2\text{O}_3\text{-TiO}_2$  and  $\text{Cr}_3\text{C}_2\text{-NiCr}$ , respectively, as compared to  $1.74 \times 10^{-5} \text{ mm}^3/\text{Nm}$  for an uncoated GCI brake rotor. Bekir et al. [94] studied the braking performance of an APS  $\text{Cr}_2\text{O}_3\text{-}40\%\text{TiO}_2$  coated cast iron brake disc compared to an uncoated disc. Results showed that the hardness of the coated disc was three times greater than that of the uncoated disc. The former also displayed a significantly reduced weight loss than the uncoated disc with the brake lining wear remaining largely unchanged, as shown in Figure 5. The dynamometer tests also showed good stability and improvement in CoF of the coated disc ( $\sim 0.49$ ) compared with the uncoated disc ( $\sim 0.56$ ). More recently, Abhinav et al. [95] studied the corrosion resistance of  $\text{Al}_2\text{O}_3 + \text{ZrO}_2\text{-}5\text{CaO}$  coatings sprayed by APS on GCI substrate. Salt spray test results showed negligible weight loss in case of all coating systems sprayed with different top coat thickness.

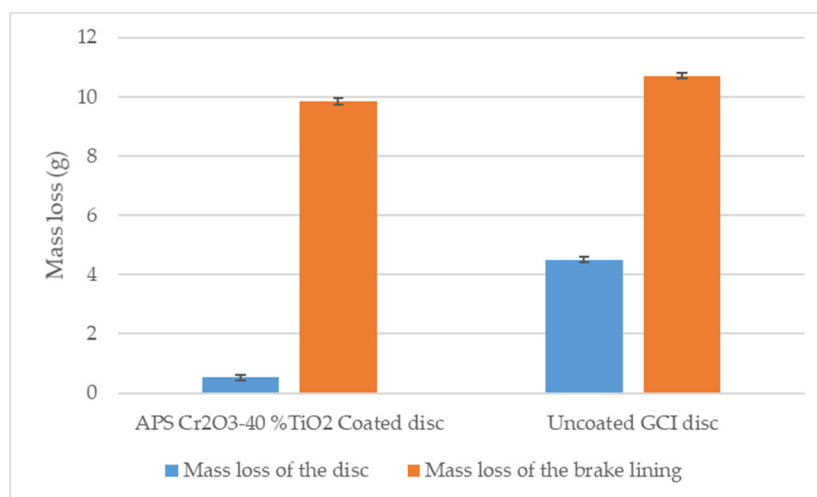


**Figure 5.** Comparative mass loss of APS Cr<sub>2</sub>O<sub>3</sub>-40%TiO<sub>2</sub> coated and uncoated GCI brake discs and corresponding brake lining mass loss, adopted from Bekir et al. [94].

Despite their widespread industrial adoption, one prominent drawback of APS coatings is that the sprayed layers usually contain defects, such as high porosity, cracks, and in situ formed oxides trapped between splats which can affect coating properties [96–100]. Moreover, the adhesion of APS coatings thicker than 0.5 mm is typically found to be poor and the high temperature of plasma jet can result in thermal damage to the powder feedstock (e.g., carbide decarburization, elemental loss, or excessive oxidation of the coating) [96,98,101]. Due to these concerns, there remains much scope for further improvements in coating quality when it comes to spraying of highly dense and corrosion resistant coatings for brake discs.

### 2.2.2. High Velocity Oxy-Fuel (HVOF)

HVOF is a widely used thermal spray process both commercially as well as for research purposes wherein raw powder particles are injected in a spray gun and accelerated by a high temperature supersonic gas stream to produce dense coatings [102]. Typical flame temperature in HVOF is around 3000 °C which is sufficient to melt the metallic powders and semi-melt the cermet feedstock powder [103]. Propane is the most commonly used fuel for combustion, although fuels such as propylene, acetylene, methane, kerosene, and their combinations have also been used [104]. The size of feedstock powder particles is typically in the range of 10–63 µm and the particles can attain velocities up to 800 m/s [104,105]. The process is commonly employed for depositing metal and cermet coatings with very low porosity, high hardness, good cohesive and adhesive strength, along with excellent wear resistance [102,106]. The process has also proven to be capable of providing coatings which can be a promising replacement for conventional hard chrome plating. The HVOF technique has been used prominently with WC-Co and WC-CoCr exhibiting superior wear resistance [107,108] and is currently the process of choice for a vast majority of industrial wear applications. Coating of other cermets like Cr<sub>3</sub>C<sub>2</sub>-NiCr [109,110], Cr<sub>3</sub>C<sub>2</sub>-WC-FeCoNi [111], as well as iron alloy-based powders [112,113] have also shown promising results in terms of wear resistance. Although a risk of decarburization of fine powder particles due to overheating [106,114] and formation of brittle carbide phases which can often result in crack formation [115] have also been reported, the extent is much lower than that observed in the case of APS [116].

The encouraging results obtained by HVOF spraying have expectedly prompted several efforts aimed at addressing brake disc applications. In a study carried out by Stanford et al. [6], friction and corrosion behavior of GCI discs coated with a stellite alloy powder by HVOF was compared to that of three other flame sprayed coatings, viz. Ni-17Cr-2.5Fe-2.5Si-2.5B-0.15C, Fe-30Mo-2C and Zn-50SiC. The stellite coating exhibited a lower CoF, stable friction behavior, and excellent corrosion resistance in



contrast to the flame sprayed coatings. Studies conducted by Demir et al. [92] and Samur et al. [93] discussed in Section 2.2.1 have also shown promising results for HVOF sprayed  $\text{Cr}_3\text{C}_2$ -NiCr coated brake disc in terms of lower wear rate and high corrosion resistance as compared to reference cast iron disc. Wear behavior of HVOF sprayed  $\text{Cr}_3\text{C}_2$ -NiCr coatings deposited on GCI discs was also studied by Priyan et al. [117]. Two different powder chemistries, viz.  $80\text{Cr}_3\text{C}_2$ -20NiCr and  $75\text{Cr}_3\text{C}_2$ -25NiCr, were used and the former showed the least weight loss during dry the sliding pin-on-disc test as well as lowest CoF due to its higher carbide content. Federici et al. [118,119] carried out studies on pearlitic cast iron brake discs HVOF coated with WC-10Co-4Cr and  $75\text{Cr}_3\text{C}_2$ -25NiCr. The coated brake discs exhibited a uniform wear track profile and very low wear rate at room temperature and at  $300^\circ\text{C}$  as compared to the reference cast iron brake disc when tested against a low-metallic friction pin [118]. Figure 6 shows the surface wear track profiles of the three discs after their pin-on-disc tests, which confirm good resistance to wear of the coated discs. During the laboratory tests, the wear mechanism of the WC-10Co-4Cr coating was found to change from abrasive wear to adhesive wear with reducing surface roughness ( $R_a$ ) of the coated specimens [119].

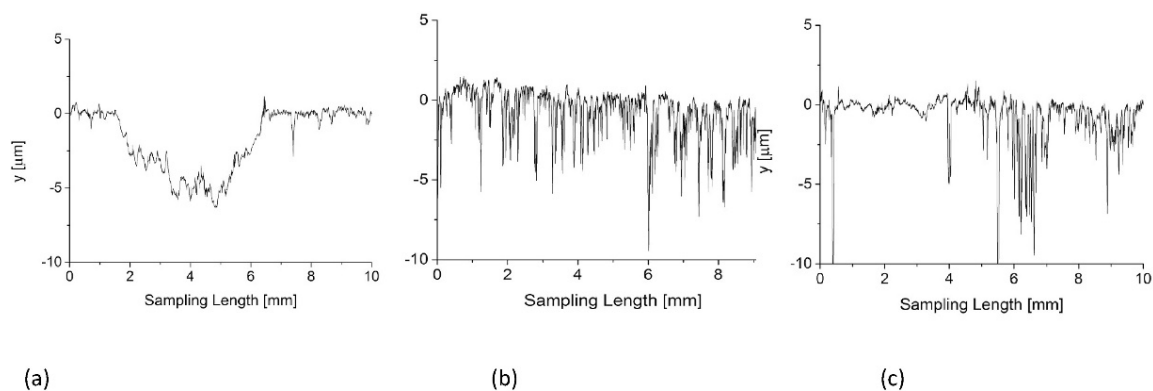


**Figure 6.** Surface wear track profiles after pin-on-disc tests at room temperature of; (a) GCI disc; (b) WC-10Co-4Cr coated disc; and (c)  $75\text{Cr}_3\text{C}_2$ -25NiCr coated disc [118]. Reprinted with permission from [118]. © 2017 Elsevier.

Öz et al. [120] compared the braking performance, noise levels, and CoF of WC-12Co HVOF coated brake discs with a GCI disc. Employing a  $50\text{ }\mu\text{m}$  bonding layer of 80Ni-20Cr under a  $500\text{ }\mu\text{m}$  thick WC-12Co coating, the coated disc exhibited higher braking performance, uniform distribution of surface temperature, lower noise levels, but slightly higher CoF than the reference GCI brake disc. A more recent study by Wahlström et al. [121] on HVOF WC-10Co-4Cr coated GCI brake disc has also yielded very encouraging results. The brake discs were tested against friction pins made from two different materials, one low-metallic and the other one with embedded  $\text{TiO}_2$  nanoparticles. In both the cases, the wear rate of the coated disc was negative, indicating that the wear debris may have transferred from the pin material on to the disc. Figure 7 shows the wear rates of the friction pairs used in this study. They also captured the particle emissions during its testing using a modified pin-on-disc tribometer, with the coated disc showing 50% reduction in particle emissions as compared to the reference GCI disc. The above reported studies abundantly reveal the promise of HVOF coatings as one of the suitable solutions for demanding brake disc applications.

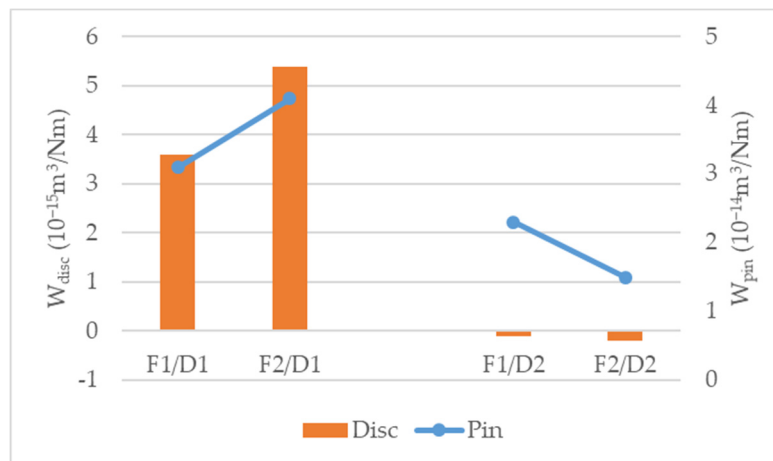


**Figure 7.** Mean specific wear rate of friction pairs in contact; F1 and F2 represent low-metallic friction material and nano-TiO<sub>2</sub> embedded friction material respectively, whereas D1 and D2 represent GCI disc and HVOF WC-10Co-4Cr coated disc respectively, adopted from Wahlström et al. [121].

### 2.2.3. Cold Gas Dynamic Spray (CGDS)

Cold gas dynamic spray (CGDS), also known as cold spray, is a process of depositing solid powder particles at very high velocities, typically in the range of 800–1200 m/s, using a convergent-divergent (de Laval) nozzle [122,123]. During its deposition, the powder particles are heated using a gas mixture of Helium (He) or Nitrogen (N<sub>2</sub>) or compressed air and propelled at the substrate. The typical size of powder particles is the range of 5–50  $\mu\text{m}$  in diameter [123]. As the name suggests, this process is characterized by low process temperature as compared to other thermal spray processes. The powder particles are well below their melting point and deform plastically on impact due to high kinetic energy thereby creating a “splat” [123]. In order for the bonding of splats to occur, the particles should have a certain impact velocity, known as critical velocity [124,125]. This critical velocity is highly dependent on the material properties [126,127] particle temperature [128], and also the substrate properties [129]. The main advantage of cold spray process is its lower process temperature which minimizes the risk of the oxidation of powder particles in-flight [130].

In a study carried out by Lima et al. [131], the brittle phases of WC-Co powders such as W<sub>2</sub>C and WO<sub>3</sub> which are formed during spraying in other high velocity thermal spray processes were not seen in the coatings sprayed by cold spray, as observed in Figure 8. Although largely limited to deposition of ductile materials, the CGDS technique has been explored for various applications, including repair. Poirier et al. [132] evaluated the wear and corrosion behaviour of a cold sprayed 300 series stainless-steel coating deposited on a Al 356-T6 brake rotor. The coating showed negligible porosity (~0.2%) as observed in Figure 9, exhibited good adhesion strength (>76 MPa) and was found to have very high corrosion resistance. Although the CoF of the coated rotor (0.38) was similar to the reference GCI rotor, its wear rate  $((4.774 \pm 1.664) \times 10^{-5} \text{ mm}^3/\text{m})$  was almost four times higher. In order to improve the wear resistance, a duplex coating with cold sprayed bond coat and arc-sprayed top coat was developed which showed very high wear resistance  $((0.751 \pm 0.067) \times 10^{-5} \text{ mm}^3/\text{m})$ .

The main limitation of this process is that it is suitable only for materials having low temperature ductility, such as metals and polymers [133]. The loss in ductility of particles through work hardening and high velocity impact may lead to formation of hard and brittle coatings which are also susceptible to cracking [132,134]. Consequently, the cold spray process is not ideally suited for deposition of carbide-based hard coatings that are relevant to dust free brake discs, although studies have reported efforts in this direction with promising results [135,136].

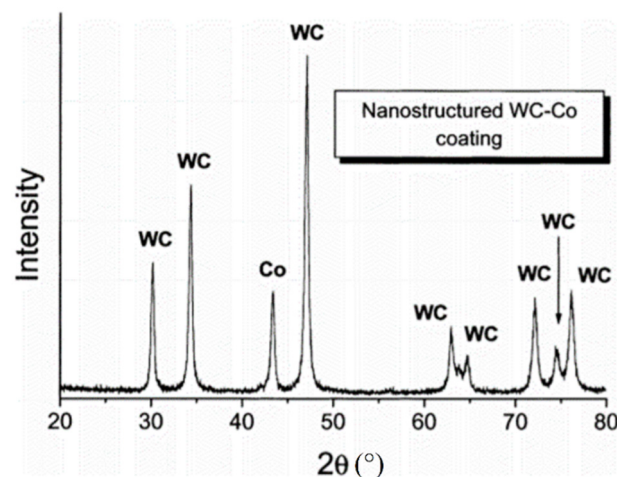


**Figure 8.** X-ray diffraction (XRD) of the nanostructured WC-12Co coating sprayed by cold spray [131]. Reprinted with permission from [131]. © 2002 Elsevier.

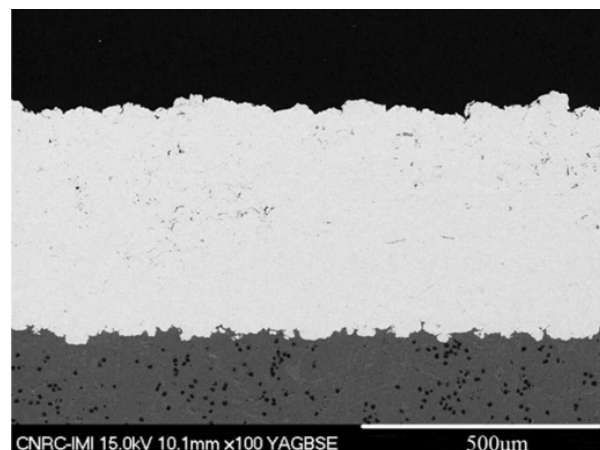


**Figure 9.** Scanning electron microscope (SEM) micrograph showing cross section of cold sprayed stainless-steel coating [132]. Reprinted with permission from [132]. © 2018 Springer Nature.

#### 2.2.4. High Velocity Air Fuel (HVOF)

In an effort to overcome the disadvantages of carbide dissolution and brittle phase formation in HVOF, the relatively new thermal spray process of high velocity air fuel (HVOF) has been attracting growing attention in the last few years [137]. The process uses air instead of oxygen which makes it colder than HVOF [138] and also has higher process velocity because of a convergent-divergent (de Laval) nozzle thereby mitigating the problems of decarburization [106,139] while simultaneously reducing the operational as well as production costs. The resulting very high particle velocities at impact, in the range of 1000–1200 m/s have been found to produce extremely dense coatings with superior cohesive and adhesive strength [140]. Therefore, HVOF coatings are deemed attractive for corrosion and wear applications and have been investigated for depositing numerous Ni- and Fe-based compositions [141–143] as well as carbide-laden coatings [144,145]. Due to these attractive features, HVOF has been increasingly explored as an alternative to the HVOF technology [84]. Although no specific work has been done on coatings solely for automotive brake discs using HVOF, several studies have been carried out on wear resistant coatings [109,113,146] that are of potential relevance to brake disc applications. Therefore, it will be of high interest to study the wear behavior of such coatings on gray cast iron brake discs.

Bolelli et al. [106] compared the sliding and abrasive wear behavior of  $\approx 300 \mu\text{m}$  thick HVOF WC-10Co-4Cr coating with an electroplated hard chromium coating having similar thickness. The highly

dense HVAF coating exhibited very low sliding and abrasive wear rate compared to electroplated hard chrome coating. Moreover, the HVAF coating also retained almost all the WC grains from the feedstock powder. Similar observations were also reported in several other studies on HVAF WC-10Co-4Cr coatings, confirming the ability of this process to limit the decarburization of WC due to the inherently lower process temperature [145–147]. As observed from Figure 10, the HVAF sprayed WC-10Co-4Cr coating had fairly similar wear rate as the HVOF coating but five times lower wear rate as compared to 300M steel substrate when tested on a reciprocating ball-on-block test against a cemented carbide counterbody, under a load of 50 N [146]. The above stated studies also highlight the favorable comparison of HVOF and HVAF processes, with HVAF sprayed coatings showing similar if not slightly better tribological behavior and corrosion resistance under similar test conditions.

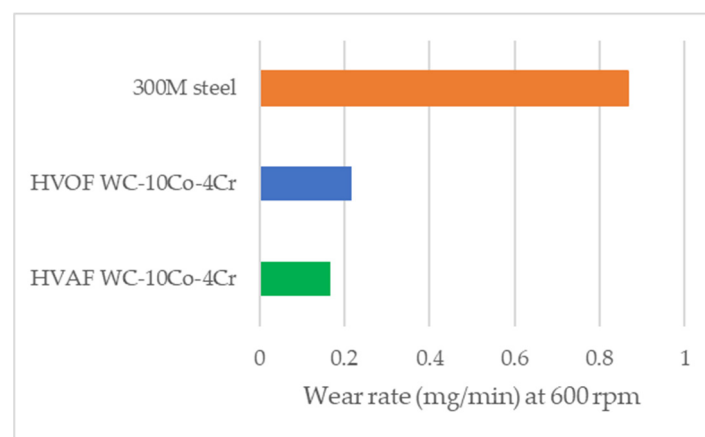


**Figure 10.** Wear rate of HVAF and HVOF WC-10Co-4Cr coating and 300M steel substrate, adopted from Liu et al. [146].

Wear behavior of CrC-based cermet coatings deposited by HVOF and HVAF was investigated by Hulka et al. [111]. They found that HVAF sprayed coatings showed slightly lower wear loss in abrasive and sliding wear tests compared to HVOF coated specimens. Bolelli et al. [110] studied the tribological behavior of HVAF  $\text{Cr}_3\text{C}_2\text{-NiCr}$  coatings at ambient temperature and at 400 °C. The coatings had a low mass loss similar to the HVOF coated samples but more than three times lower than the reference electroplated hard chrome coating. Sliding wear rate was also seen to be lower than hard chrome coated specimen but again similar to the HVOF coating for both room temperature as well as at 400 °C. The comparable results of HVOF and HVAF carbide laden coatings from above the reported studies further strengthen the case of HVAF as one of the promising candidates which can be deployed to coat automotive brake discs, particularly by virtue of its lower operating costs.

#### 2.2.5. Suspension Plasma Spray (SPS)

SPS is a relatively recent technology which uses finely grained, nanometer, sub-micrometer, and micrometric sized powder suspension as a feedstock to form the coatings [148]. The suspension is injected into the plasma jet where it atomizes, and the liquid component evaporates rapidly. Upon impact, a chain of events similar to that in APS occurs: The molten particles first splat, then rapidly solidify, and the coating is built up by successive deposition of particles [148].

SPS offers several advantages over APS. The long desire to spray sub-micron and nano-sized particles can be achieved by this process and can enable the formation of unique coating morphology that offers a dense coating with refined grains, small sized porosity, and excellent interlamellar bonding [85]. Furthermore, the recent advancement in axial suspension feeding for SPS technology has shown significant improvement in both deposition efficiency and thermal exchange between the feedstock and the plasma plume [148,149]. Recognizing the above advantages, this process has emerged as a promising spraying technique and several studies have been carried out to explore the potential of the



SPS process. SPS thermal barrier coatings have been the subject of particularly intensive investigation and, as an outcome of the numerous dedicated studies, the process is now well understood. Due to its ability to spray nano-sized particles with different solvents, the microstructure of the coatings can be tailored to produce a variety of microstructures such as porous columnar, dense vertically cracked, etc. [150–153]. Such microstructures can be further tailored to produce refined microstructures more suitable for wear resistance applications than APS coatings as evident from the results of Goel et al. [149] illustrated in Figure 11. Moreover, a preliminary work by our group to explore the potential of SPS to spray  $\text{Cr}_2\text{O}_3$  coating has shown prominent results to develop a new generation of wear resistance coatings. The cross-section micrograph of SPS  $\text{Cr}_2\text{O}_3$  demonstrates the potential of this process to deposit a dense layer of  $\text{Cr}_2\text{O}_3$  with fine porosity, as shown in Figure 12.

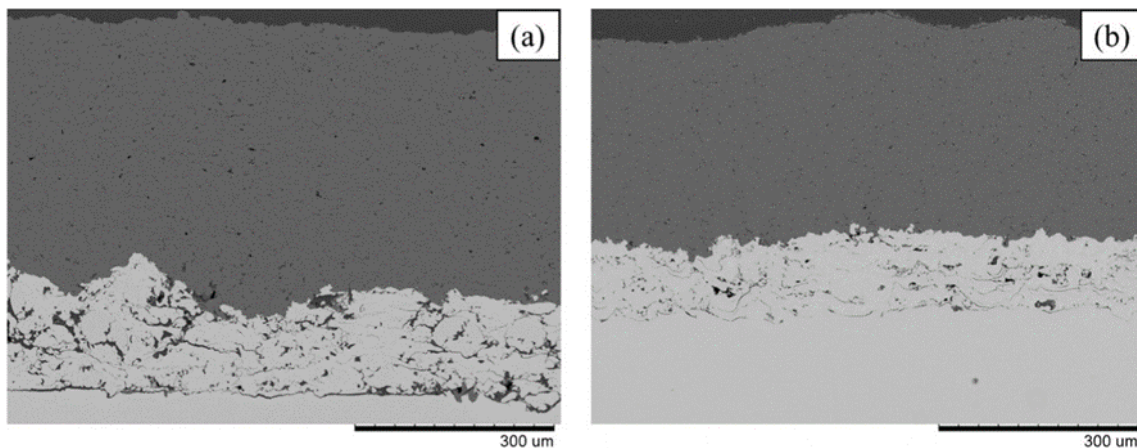


**Figure 11.** SEM image of cross section of; (a) APS  $\text{Al}_2\text{O}_3$ ; and (b) SPS  $\text{Al}_2\text{O}_3$  [149]. Reprinted with permission from [149]. © 2017 Elsevier.

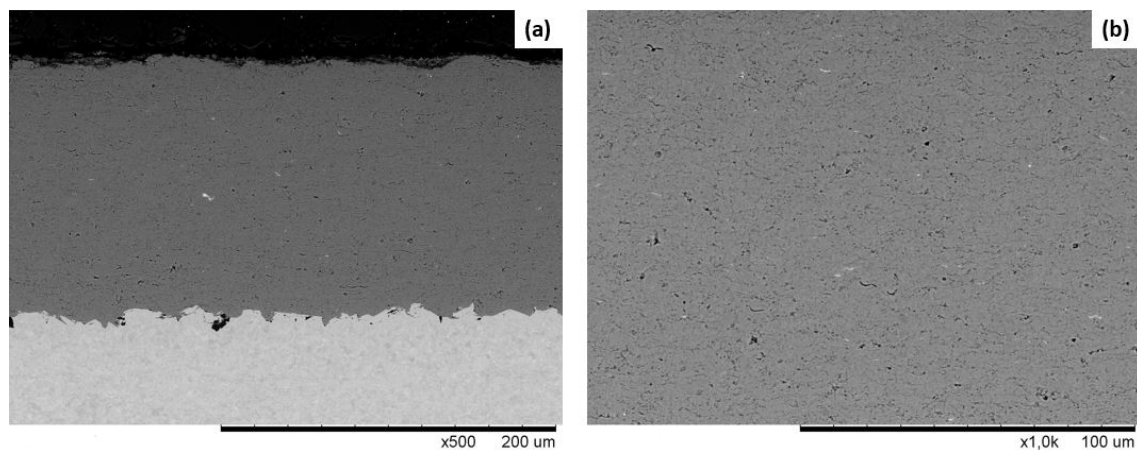


**Figure 12.** SEM image of cross section of SPS  $\text{Cr}_2\text{O}_3$  showing; (a) low magnification cross-sectional overview; and (b) high magnification microstructure with fine distributed porosity.

However, the research on SPS wear resistance coating is still incipient and very few works have been conducted [154–158]. Early results by Tingaud et al. [154] showed an improvement in the wear resistance of SPS  $\text{Al}_2\text{O}_3$  as well as low CoF ( $\sim 0.39$ ) by adding  $\text{ZrO}_2$  in the matrix.

The interest in exploring liquid-based spraying has been expanded significantly and novel methods for depositing composite, multilayered, functionally graded coating, and hybrid processes have emerged to enhance surface properties even further [159–162]. Gopal et al. [163] demonstrated the potentials of hybrid technique by combining dual injection of distinct feedstock types to offer superior wear resistance coating. Sliding test results of the hybrid coating ( $\text{Al}_2\text{O}_3$  powder with YSZ



suspension) showed a superior crack growth resistance as well as low CoF ( $\sim 0.24$ ) as compared with pure coating. However, the process has not yet been fully explored for brake disc applications despite its promising potential.

From the review of literature carried out, thermal spray variants bear promises to be applied on GCI brake discs and, in the near future, also keep pace with the regulatory demands that are certain to become increasingly stringent. These methods are amenable to spraying coatings over a wide range of thickness and on parts with complex geometries. The versatility that is derived from the capability to spray a wide range of materials such as metals, cermets, ceramics, as well as composites also offers a unique opportunity to move towards producing coatings for GCI brake discs that would reduce dust and emissions due to brake wear.

### 3. Coating Materials

There is a large range of potential materials that can be deposited by the previously discussed thermal spray techniques for wear resistant applications. The following section summarizes an exhaustive survey of available literature to identify materials that have been applied on actual brake discs or on gray cast iron substrates and other materials deemed promising for wear resistant application. Both materials deployed in actual applications, as well as those that have yielded promising laboratory test results (in terms of low CoF and wear rate) have been considered in the ensuing discussion. The materials have been categorized based on their composition into three major groups; (i) oxides, (ii) carbides, and (iii) alternative materials.

#### 3.1. Oxides

Aluminum oxide ( $\text{Al}_2\text{O}_3$ ), titanium oxide ( $\text{TiO}_2$ ) and chromium oxide ( $\text{Cr}_2\text{O}_3$ ) are widely used materials for tribological applications requiring both wear and corrosion resistance [164–166]. The oxide ceramics materials in general have shown high strength, hardness and good wear and corrosion resistance [167–171]. APS has been the most commonly used thermal spray technology to deposit these materials due to their high melting temperature [164,165,167]. Numerous studies have been carried out to investigate the mechanical and wear resistant property of plasma sprayed ceramic oxides [164,172–184].

Several researchers have investigated the potential of these materials to impart improved wear resistance on brake discs by plasma spraying. Some of these studies have been discussed in Section 2.2.1. Yet other efforts have focused on such ceramic-based APS coatings deposited on cast iron substrates and studied their tribological behavior. Both of the above are summarized below in Table 3.

**Table 3.** Summary of sliding wear studies involving oxide-based coatings on brake discs and cast-iron substrates.

Coating Process	Coating Material	Substrate	Coating Hardness	CoF	Counter Body	Ref.
APS	$\text{Ti}_n\text{O}_{2n-1}$ ( $n = 4-6$ )	GCI	846 HV0.2	0.58–0.78	Sintered $\text{Al}_2\text{O}_3$ ball	[90]
APS	8YSZ $\text{ZrO}_2$ 75Cr <sub>3</sub> C <sub>2</sub> -25NiCr	4130 steel brake discs	– 1400 HV0.2 800 HV0.2	0.55 0.65 0.35	Fe-Cu pad	[91]
APS	$\text{Al}_2\text{O}_3$ - $\text{TiO}_2$	GCI brake disc	–	0.27	As per SAE J2522 dynamometer test	[92]
APS	$\text{Cr}_2\text{O}_3$ -40% $\text{TiO}_2$	GCI brake disc	842 HV0.5	0.49	As per SAE J2522 dynamometer test	[94]
APS	$\text{Cr}_2\text{O}_3$	Cast iron	1200 HV0.1	0.60	Self-mated $\text{Cr}_2\text{O}_3$ -coated discs	[180]
APS	$\text{Cr}_2\text{O}_3$ -5MoO <sub>3</sub>	Cast iron	1700 HV0.1	0.40	Cr-plated disc	[175]

Table 3. Cont.

Coating Process	Coating Material	Substrate	Coating Hardness	CoF	Counter Body	Ref.
APS	Al <sub>2</sub> O <sub>3</sub>	Cast iron	1150 HV0.3	0.45–0.55	D2 steel disc	[185]
APS	8YSZ	Cast iron	980 HV0.1	0.85	Cr-plated disc	[186]
	20YSZ		450 HV0.1	0.90		
	ZrO <sub>2</sub> + 5CaO		300 HV0.1	0.80–0.55		
	Al <sub>2</sub> O <sub>3</sub> -ZrO <sub>2</sub>		960 HV0.1	0.80–0.70		
APS	Mo	Cast iron	500 HV0.1	–	AISI 303 steel pin	[187]

Although not included in the above table, SPS wear resistant coatings appear promising to investigate for brake disc application owing to their potential of utilizing the advantages of sub-micron and nanometric powder particles. The encouraging results obtained by SPS wear resistant coatings have already been highlighted in Section 2.2.5 and further investigations on the same front also demonstrate the ability of this process to produce superior wear resistant coatings [188].

### 3.2. Carbides

Hard metal carbides such as tungsten carbide (WC) and chromium carbide (Cr<sub>3</sub>C<sub>2</sub>) bonded with pure metal or mixture of metals consisting of cobalt (Co), nickel (Ni), chromium (Cr), iron (Fe) are one of the most frequently used cermets for producing highly wear resistant coatings by high velocity thermal spray processes [189–191]. These cermets, also referred to as cemented carbides, have an optimum blend of hardness, toughness, and ductility which makes them attractive for applications that demand materials having high wear and corrosion resistance [192]. Currently, high velocity thermal spray processes of HVOF and HVOF are acknowledged to be the most appropriate processes for spraying cemented carbides. The lower oxide content in deposited coatings due to low process temperatures and short residence times due to supersonic gas stream results in good cohesion and adhesion along with reduced porosity and low decarburization [193,194]. The carbide dissolution can be reduced significantly by using HVOF which has an even lower process temperature than HVOF [138].

Several studies on sliding wear and thermal properties of HVOF sprayed carbide coatings on brake discs have been carried out in the past. Among the hard metal carbides, WC-12Co, WC-10Co-4Cr and 75Cr<sub>3</sub>C<sub>2</sub>-25NiCr have been the most popular for realizing highly wear resistant coatings. The most notable efforts involving carbide coatings on brake discs using HVOF technique has been previously discussed in Section 2.2.2. Table 4 below summarizes the various studies reported on carbide coatings on cast-iron brake discs.

Apart from these studies on brake discs, such hard metal HVOF carbide coatings have also been used extensively in other industrial applications to study their wear and corrosion resistance. Du et al. [195] compared the wear rate of plasma sprayed WC-12Co coating on GCI substrates using a lubricated ball on disc tribometer. They found that, although the CoF of the coating was similar to bare GCI substrate, volume loss in case of bare GCI was six times higher than that with plasma sprayed coating. Several comparative studies on tribological properties of thermally sprayed carbide coatings have also been carried out in the past using HVOF and/or HVOF [106,110,111,137,146,196]. From these studies, the carbide-based HVOF coatings have proven to be superior than HVOF in terms of their wear resistance and the ability to retain the feedstock carbide grains. The results of various HVOF tribological coatings reported in Section 2.2.4 have shown extremely promising results in different wear tests and therefore make a strong case to be explored specifically for brake disc application.

**Table 4.** Summary of sliding wear studies involving carbide coatings on brake discs.

Coating Process	Coating Material	Substrate	Coating Hardness	CoF	Counter Body	Ref.
HVOF	Co-30Cr-12W-2.4C	Gray cast iron	812 HV0.3	0.30–0.35	Non-asbestos organic (NAO) brake pad material	[6]
HVOF	75Cr <sub>3</sub> C <sub>2</sub> -25NiCr	Gray cast iron	766 HV0.2	0.29–0.36	As per SAE J2522 dynamometer test	[92]
HVOF	75Cr <sub>3</sub> C <sub>2</sub> -25NiCr	Gray cast iron	766 HV0.2	–	10 mm diameter Al <sub>2</sub> O <sub>3</sub> ball	[93]
HVOF	80Cr <sub>3</sub> C <sub>2</sub> -20NiCr	Gray cast iron	1410 HV0.3	0.20–0.24	WC-6Co pin	[117]
HVOF	86WC-10Co-4Cr	Cast iron	1100 HV0.3	0.48–0.49	Commercial low-metallic friction material	[119]
HVOF	75Cr <sub>3</sub> C <sub>2</sub> -25NiCr	Pearlitic cast iron	920 HV0.3	0.43–0.59	Commercial low-metallic friction material	[118]
HVOF	86WC-10Co-4Cr	Pearlitic cast iron	1130 HV0.3	0.30–0.66	Commercial low-metallic friction material	[118]
HVOF	88WC-12Co	Gray cast iron	510 HV0.2	0.51–0.52	Low-metallic friction material	[120]
HVOF	86WC-10Co-4Cr	Cast iron	–	0.48–0.49	Experimental	[121]

### 3.3. Alternative Materials

Over the last decade, the prices of Ni and Co have increased dramatically and forced the thermal spray community to evaluate alternative materials for wear-resistance applications [197,198]. Moreover, metals and/or compounds of metals like Ni, Co, hexavalent Cr, and specifically WC-Co-based powders have been identified as human carcinogens by the International Agency for Research on Cancer and by the U.S. Department of Health and Human Services [199], especially in inhalable form [200]. There is also a risk of fine wear debris being released when these materials are used in the form of a coating. This has further motivated the search for economical and environmentally sustainable alternative materials that are either free of the above elements or at least reduce their content.

Preliminary studies on economically more appealing stellite alloy coatings or self fluxing Ni-Cr-B-Si alloy coatings with a Fe matrix have shown promising results [112,201]. Moreover, recent work on tribological properties of a novel coating sprayed using Fe-V-Cr-C alloy system with HVOF and HVAF have shown that these coatings yield results comparable with stellites and Ni-Cr-B-Si alloys [113,202]. Hence, Fe-based coatings are a promising alternative to Ni/Co-based coatings due to their lower toxicity as well as lower cost. Another alternative material, WC-FeCrAl, termed as a “green carbide” due to the Fe-based matrix replacing Ni and/or Co as the binder, is also a potential replacement for WC-Ni/Co carbide powders. Bolelli et al. [203] studied the sliding wear resistance of WC-FeCrAl coatings sprayed by HVOF and the results showed its sliding wear performance to be comparable to WC-Co-Cr coating. A comparative study of HVOF and HVAF sprayed WC-FeCrAl coatings was also carried out by Bolelli et al. [204] where both the coatings showed very similar wear rates at room temperature and at 400 °C. In another study conducted by Brezinová et al. [205], HVOF sprayed WC-FeCrAl coatings showed excellent erosive and abrasive wear resistance as well as good corrosion resistance.

A summary of the inherent thermo-physical properties of some of the promising oxide, carbide, and alternative materials that could be candidates for actual brake disc applications is provided in Table 5.

**Table 5.** Summary of promising coating materials for brake disc application.

Material	Bulk Density (g/cm <sup>3</sup> )	Thermal Conductivity (W/m.K (°C))	Thermal Expansion Coefficient (K <sup>-1</sup> × 10 <sup>-6</sup> )	Vickers Hardness (HV)	Ref.
Al <sub>2</sub> O <sub>3</sub>	3.65–3.96	30–36	4.50–8.30	1520–1680	[20]
Cr <sub>2</sub> O <sub>3</sub>	4.20–4.40	10–33	7.80–8.10	1280–1420	[20]
Fe-V-Cr-C alloy	7.50	–	–	800–950	[113]

Table 5. Cont.

Material	Bulk Density (g/cm <sup>3</sup> )	Thermal Conductivity (W/m.K (°C))	Thermal Expansion Coefficient (K <sup>-1</sup> × 10 <sup>-6</sup> )	Vickers Hardness (HV)	Ref.
WC-FeCrAl	14.42	–	6.17–6.68	950–1200	[204,205]
75Cr <sub>3</sub> C <sub>2</sub> -25NiCr	7	14	11.10	1350	[206]
WC-17Co	14.54	81.50	–	1060–1170	[207]

#### 4. Industrial Implications

The automotive industry is constantly in need of new materials and developments in order to sustain their fast-developing business [76]. New standards and regulations that will emerge in few years' time concerning PM emissions from automobile brake wear are certain to force the automotive industries to actively seek approaches for minimizing or eliminating particle emissions. Another factor that would drive the global automotive brake market is the emergence of electric vehicles (EVs) and hybrid vehicles. Braking systems for EVs mainly rely on the principle of regenerative braking, which implies that the conventional frictional braking system is less frequently used. A regenerative braking system enables the kinetic energy of the drive wheels to be converted to electrical energy by the electric motor (generator) during braking, deceleration, or downhill running [208]. The converted electrical energy, which is normally lost as frictional heat, is stored in energy storage devices such as high voltage batteries, ultracapacitors, and ultrahigh-speed flywheels to extend the driving range by up to 10% [209]. However, regenerative braking is not self-sufficient as the only means to bring a vehicle to a stop, for instance, during emergency braking. It is, therefore, usually used in combination with a friction braking system [210]. Therefore, an electric motor (generator) brake and an electric-hydraulic composite braking system are adopted for electric vehicles braking systems [211]. Since friction brakes are less frequently used as in traditional vehicles due to regeneration properties [212], the problem of corrosion will also be prominent if GCI disc rotors are used, with the fundamental property requirements placed on friction brakes remaining unchanged in EVs. Thus, the major factors that could influence the application of friction brakes in EVs are the demand to reduce the vehicle's weight, reduce particle emissions due to wear, and the requirement to prevent brake disc corrosion.

Concerns regarding non-exhaust PM emissions will also be prevalent in the near future because the exhaust PM emissions would have been eliminated or considerably reduced due to electrification of vehicles [29]. However, for GCI brake discs to be relevant in this era, drastic measures to improve their corrosion and wear properties must be taken by the automotive component manufacturers. The use of thermal spray processes to deposit highly wear resistant coatings on GCI brake discs can go a long way in reducing the brake dust as well as other emissions from brake wear. Such encouraging results have been already demonstrated by using HVOF in a recent study [121].

These results can be further improved by using emergent and state of the art technologies such as HVAF and SPS. If these methods are developed to their full capability, they can potentially form a robust coating platform to enable the automotive industry to address aforementioned problems while achieving their sustainability goals as well as satisfying brake disc requirements [76,105]. Moreover, the coated brake discs will also have higher durability that will indirectly lower the maintenance and repair costs associated with them. New markets for thermal spray will also be opened which could not only bring down the operational and production costs of these processes but also increase their economic value simultaneously [76]. This will drive the global automobile brake disc market in the coming years.

#### 5. Conclusions

Brake wear emissions in the form of brake dust and particulate matter are a growing concern for the automotive industry since they significantly contribute to increasing traffic pollution, and can also pose a challenge in the face of increasingly stringent standards and environmental norms. As GCI continues to be the primary brake disc material of choice for passenger vehicles, surface treatment of GCI discs

offers a possible pathway to address the above challenge. This paper comprehensively reviews various candidate coating techniques and materials that have been traditionally used/evaluated to mitigate brake wear emissions. Among them, thermally sprayed coatings are noted to provide specific benefits. Several illustrative examples of thermal spray coatings deposited on GCI substrates and/or specifically investigated for possible brake disc applications have been presented. Compared to conventional techniques like APS and HVOF, development of anti-wear and anti-corrosive coatings by deploying emergent thermal spray variants such as HVAF and SPS can potentially lead to direct payback in terms of improved air quality along with enhanced life of brake discs. The benefits that these two methods offer compared to the relatively more well-established techniques are outlined, and the industrial implications of adopting them for brake disc applications, have been discussed. A summary of promising oxide, carbide, and alternative materials that could be candidates for actual brake disc applications, is also included. A focused effort aimed at evaluating these promising spray process-coating material combinations can lead to important tangible outcomes for the automotive industry.

**Author Contributions:** Conceptualization, S.A. and S.J.; Validation, O.A., W.A. and S.J.; Formal Analysis, S.J.; Investigation, S.J.; Data Curation, O.A. and S.J.; Writing—Original Draft Preparation, O.A., W.A. and S.A.; Writing—Review and Editing, O.A. and S.J.; Project Administration, S.A. and S.J.; Funding Acquisition, S.J.

**Funding:** Financial assistance from Energimyndigheten, Sweden (Project Number 46393-1) for the NUCoP Project which enabled this study is gratefully appreciated.

**Acknowledgments:** The authors would like to acknowledge all the project partners and colleagues for their valuable inputs and discussion on the manuscript.

**Conflicts of Interest:** The authors declare no conflict of interest.

## References

1. Rashid, A. Overview of disc brakes and related phenomena—A review. *Int. J. Veh. Noise Vib.* **2014**, *10*, 257–301. [\[CrossRef\]](#)
2. Cueva, G.; Sinatora, A.; Guesser, W.L.; Tschiptschin, A.P. Wear resistance of cast irons used in brake disc rotors. *Wear* **2003**, *255*, 1256–1260. [\[CrossRef\]](#)
3. Thornton, R.; Slatter, T.; Jones, A.H.; Lewis, R. The effects of cryogenic processing on the wear resistance of grey cast iron brake discs. *Wear* **2011**, *271*, 2386–2395. [\[CrossRef\]](#)
4. Cho, M.H.; Kim, S.J.; Basch, R.H.; Fash, J.W.; Jang, H. Tribological study of gray cast iron with automotive brake linings: The effect of rotor microstructure. *Tribol. Int.* **2003**, *36*, 537–545. [\[CrossRef\]](#)
5. Shin, M.W.; Cho, K.H.; Kim, S.J.; Jang, H. Friction instability induced by corrosion of gray iron brake discs. *Tribol. Lett.* **2010**, *37*, 149–157. [\[CrossRef\]](#)
6. Stanford, M.K.; Jain, V.K. Friction and wear characteristics of hard coatings. *Wear* **2001**, *251*, 990–996. [\[CrossRef\]](#)
7. Maleque, M.A.; Dyuti, S.; Rahman, M.M. Material selection method in design of automotive brake disc. In Proceedings of the World Congress on Engineering 2010, London, UK, 30 June–2 July 2010; Volume III, p. 5.
8. Hjortenkrans, D.S.T.; Bergbäck, B.G.; Häggerud, A.V. Metal emissions from brake linings and tires: Case studies of Stockholm, Sweden 1995/1998 and 2005. *Environ. Sci. Technol.* **2007**, *41*, 5224–5230. [\[CrossRef\]](#)
9. Iijima, A.; Sato, K.; Yano, K.; Kato, M.; Kozawa, K.; Furuta, N. Emission factor for antimony in brake abrasion dusts as one of the major atmospheric antimony sources. *Environ. Sci. Technol.* **2008**, *42*, 2937–2942. [\[CrossRef\]](#)
10. Furusjö, E.; Sternbeck, J.; Cousins, A.P. PM10 source characterization at urban and highway roadside locations. *Sci. Total Environ.* **2007**, *387*, 206–219. [\[CrossRef\]](#)
11. Rahman, M.M.; Adebisi, A.A.; Maleque, M.A. Metal matrix composite brake rotor: Historical development and product life cycle analysis. *Int. J. Automot. Mech. Eng.* **2011**, *4*, 471–480.
12. Kim, S.W.; Park, K.; Lee, S.H.; Kang, K.H.; Lim, K.T. Thermophysical properties of automotive metallic brake disk materials. *Int. J. Thermophys.* **2008**, *29*, 2179–2188. [\[CrossRef\]](#)
13. Nakanishi, H.; Kakihara, K.; Nakayama, A.; Murayama, T. Development of aluminum metal matrix composites (Al-MMC) brake rotor and pad. *JSAE Rev.* **2002**, *23*, 365–370. [\[CrossRef\]](#)



14. Renz, R.; Seifert, G.; Krenkel, W. Integration of CMC brake disks in automotive brake systems. *Int. J. Appl. Ceram. Technol.* **2012**, *9*, 712–724. [\[CrossRef\]](#)
15. Blau, P.J.; Jolly, B.C.; Qu, J.; Peter, W.H.; Blue, C.A. Tribological investigation of titanium-based materials for brakes. *Wear* **2007**, *263*, 1202–1211. [\[CrossRef\]](#)
16. Hutton, T.J.; McEnaney, B.; Crelling, J.C. Structural studies of wear debris from carbon-carbon composite aircraft brakes. *Carbon N. Y.* **1999**, *37*, 907–916. [\[CrossRef\]](#)
17. Jang, G.H.; Cho, K.H.; Park, S.B.; Lee, W.G.; Hong, U.S.; Jang, H. Tribological properties of C/C-SiC composites for brake discs. *Met. Mater. Int.* **2010**, *16*, 61–66. [\[CrossRef\]](#)
18. Krenkel, B.W.; Heidenreich, B.; Renz, R. C/C-SiC Composites for advanced friction systems. *Adv. Eng. Mater.* **2002**, *4*, 427–436. [\[CrossRef\]](#)
19. Zuber, C.; Heidenreich, B. Development of a net shape manufacturing method for ventilated brake discs in single piece design. *Materwiss. Werksttech.* **2006**, *37*, 301–308. [\[CrossRef\]](#)
20. Edupack, C.E. *Granta Design Limited*; Cambridge: England, UK, 2005.
21. Roubicek, V.; Raclavska, H.; Juchelkova, D.; Filip, P. Wear and environmental aspects of composite materials for automotive braking industry. *Wear* **2008**, *265*, 167–175. [\[CrossRef\]](#)
22. Breuer, B.; Bill, K.H. *Brake Technology Handbook*; SAE International: Warrendale, PA, USA, 2008; ISBN 9780768017878.
23. Katsouyanni, K.; Touloumi, G.; Samoli, E.; Gryparis, A.; Le Tertre, A.; Monopolis, Y.; Rossi, G.; Zmirou, D.; Ballester, F.; Boumghar, A.; et al. Confounding and effect modification in the short-term effects of ambient particles on total mortality: Results from 29 european cities within the APHEA2 project. *Epidemiology* **2001**, *12*, 521–531. [\[CrossRef\]](#)
24. Zeger, S.L.; Samet, J.M.; Curriero, F.C.; Coursac, I.; Dominici, F. Fine particulate air pollution and mortality in 20 U.S. cities, 1987–1994. *N. Engl. J. Med.* **2002**, *343*, 1742–1749.
25. Pope, C.A., III; Burnett, R.T.; Thun, M.J.; Calle, E.E.; Krewski, D.; Ito, K.; Thurston, G.D. Lung cancer, cardiopulmonary mortality, and long-term exposure to fine particulate air pollution. *JAMA* **2002**, *287*, 1132–1141. [\[CrossRef\]](#)
26. Harrison, R.M.; Jones, A.M.; Gietl, J.; Yin, J.; Green, D.C. Estimation of the contributions of brake dust, tire wear, and resuspension to nonexhaust traffic particles derived from atmospheric measurements. *Environ. Sci. Technol.* **2012**, *46*, 6523–6529. [\[CrossRef\]](#)
27. Sharaf, J. Exhaust emissions and its control technology for an internal combustion engine. *Int. J. Eng. Res. Appl.* **2013**, *3*, 947–960.
28. Hagino, H.; Oyama, M.; Sasaki, S. Airborne brake wear particle emission due to braking and accelerating. *Wear* **2015**, *334–335*, 44–48. [\[CrossRef\]](#)
29. Grigoratos, T.; Martini, G. Brake wear particle emissions: A review. *Environ. Sci. Pollut. Res.* **2015**, *22*, 2491–2504. [\[CrossRef\]](#)
30. Bolelli, G.; Cannillo, V.; Lusvarghi, L.; Riccò, S. Mechanical and tribological properties of electrolytic hard chrome and HVOF-sprayed coatings. *Surf. Coat. Technol.* **2006**, *200*, 2995–3009. [\[CrossRef\]](#)
31. Gibb, H.J.; Lees, P.S.J.; Pinsky, P.F.; Rooney, B.C. Clinical findings of irritation among chromium chemical production workers. *Am. J. Ind. Med.* **2000**, *38*, 127–131. [\[CrossRef\]](#)
32. Occupational Safety and Health Administration (OSHA). Occupational exposure to hexavalent chromium. Final rule. *Fed. Regist.* **2006**, *71*, 10099.
33. Flitney, B. Alternatives to chrome for hydraulic actuators. *Seal. Technol.* **2007**, *2007*, 8–12. [\[CrossRef\]](#)
34. Directive, E.U. Directive 2000/53/ec of the european parliament and of the council of 18 September 2000 on end-of life vehicles. *Off. J. Eur. Union* **2000**, *269*, 34–43.
35. Mandich, N.V.; Snyder, D.L. Electrodeposition of chromium. In *Modern Electroplating*; Schlesinger, M., Paunovic, M., Eds.; Wiley: Hoboken, NJ, USA, 2010; pp. 205–241. ISBN 9781118063149.
36. Tyler, J.M. Automotive applications for chromium. *Met. Finish.* **1995**, *93*, 11–14. [\[CrossRef\]](#)
37. Bolelli, G.; Giovanardi, R.; Lusvarghi, L.; Manfredini, T. Corrosion resistance of HVOF-sprayed coatings for hard chrome replacement. *Corros. Sci.* **2006**, *48*, 3375–3397. [\[CrossRef\]](#)
38. Houdková, Š.; Zahálka, F.; Kašparová, M.; Berger, L.-M.; Houdková, S.; Zahálka, F.; Kašparová, M.; Berger, L.-M. Comparative study of thermally sprayed coatings under different types of wear conditions for hard chromium replacement. *Tribol. Lett.* **2011**, *43*, 139–154. [\[CrossRef\]](#)

39. Balamurugan, G.M.; Duraiselvam, M.; Anandakrishnan, V. Comparison of high temperature wear behaviour of plasma sprayed WC-Co coated and hard chromium plated AISI 304 austenitic stainless steel. *Mater. Des.* **2012**, *35*, 640–646. [[CrossRef](#)]
40. Lal, R.; Singh, R.C. Experimental comparative study of chrome steel pin with and without chrome plated cast iron disc in situ fully flooded interface lubrication. *Surf. Topogr. Metrol. Prop.* **2018**, *6*, 035001. [[CrossRef](#)]
41. Krelling, A.P.; Souza, M.M.D.; Costa, C.E.D.; Milan, J.C.G. HVOF-sprayed coating over AISI 4140 steel for hard chromium replacement. *Mater. Res.* **2018**, *21*, 3–12. [[CrossRef](#)]
42. Dunleavy, C.S.; Golosnoy, I.O.; Curran, J.A.; Clyne, T.W. Characterisation of discharge events during plasma electrolytic oxidation. *Surf. Coat. Technol.* **2009**, *203*, 3410–3419. [[CrossRef](#)]
43. Curran, J.A.; Clyne, T.W. Porosity in plasma electrolytic oxide coatings. *Acta Mater.* **2006**, *54*, 1985–1993. [[CrossRef](#)]
44. Tian, J.; Luo, Z.; Qi, S.; Sun, X. Structure and antiwear behavior of micro-arc oxidized coatings on aluminum alloy. *Surf. Coat. Technol.* **2002**, *154*, 1–7. [[CrossRef](#)]
45. Nie, X.; Meletis, E.I.; Jiang, J.C.; Leyland, A.; Yerokhin, A.L.; Matthews, A. Abrasive wear/corrosion properties and TEM analysis of  $\text{Al}_2\text{O}_3$  coatings fabricated using plasma electrolysis. *Surf. Coat. Technol.* **2002**, *149*, 245–251. [[CrossRef](#)]
46. Yerokhin, A.L.; Nie, X.; Leyland, A.; Matthews, A. Characterisation of oxide films produced by plasma electrolytic oxidation of a Ti-6Al-4V alloy. *Surf. Coat. Technol.* **2000**, *130*, 195–206. [[CrossRef](#)]
47. Curran, J.A.; Clyne, T.W. The thermal conductivity of plasma electrolytic oxide coatings on aluminium and magnesium. *Surf. Coat. Technol.* **2005**, *199*, 177–183. [[CrossRef](#)]
48. Alnaqi, A.; Shresha, S.; Brooks, P.C.; Barton, D. Barton david thermal performance of peo coated lightweight. In *EuroBrake 2014, Proceedings of the EuroBrake 2014 Conference, Lille, France, 13–15 May 2014*; FISITA: Lille, France, 2014.
49. Alnaqi, A.A.; Kosarieh, S.; Barton, D.C.; Brooks, P.C.; Shrestha, S. Material characterisation of lightweight disc brake rotors. *Proc. Inst. Mech. Eng. Part L J. Mater. Des. Appl.* **2018**, *232*, 555–565. [[CrossRef](#)]
50. Tsai, D.-S.; Chou, C.-C. Review of the soft sparking issues in plasma electrolytic oxidation. *Metals* **2018**, *8*, 105. [[CrossRef](#)]
51. Clyne, T.W.; Troughton, S.C. A review of recent work on discharge characteristics during plasma electrolytic oxidation of various metals. *Int. Mater. Rev.* **2018**, *64*, 127–162. [[CrossRef](#)]
52. Stojadinović, S.; Vasilčić, R.; Perić, M. Investigation of plasma electrolytic oxidation on valve metals by means of molecular spectroscopy—a review. *RSC Adv.* **2014**, *4*, 25759–25789. [[CrossRef](#)]
53. Wang, J.; Yang, W.; Ke, P.; Li, J.; Xu, D. Microstructure and properties of duplex coatings on magnesium alloy. *Surf. Eng.* **2016**, *32*, 601–606.
54. Rama Krishna, L.; Poshal, G.; Jyothirmayi, A.; Sundararajan, G. Compositionally modulated CGDS + MAO duplex coatings for corrosion protection of AZ91 magnesium alloy. *J. Alloys Compd.* **2013**, *578*, 355–361. [[CrossRef](#)]
55. Van Acker, K.; Vanhoyweghen, D.; Persoons, R.; Vangrunderbeek, J. Influence of tungsten carbide particle size and distribution on the wear resistance of laser clad WC/Ni coatings. *Wear* **2005**, *258*, 194–202. [[CrossRef](#)]
56. Fallah, V.; Alimardani, M.; Corbin, S.F.; Khajepour, A. Impact of localized surface preheating on the microstructure and crack formation in laser direct deposition of Stellite 1 on AISI 4340 steel. *Appl. Surf. Sci.* **2010**, *257*, 1716–1723. [[CrossRef](#)]
57. Zhou, S.; Zeng, X.; Hu, Q.; Huang, Y. Analysis of crack behavior for Ni-based WC composite coatings by laser cladding and crack-free realization. *Appl. Surf. Sci.* **2008**, *255*, 1646–1653. [[CrossRef](#)]
58. Nowotny, S.; Techel, A.; Luft, A.; Reitzenstein, W. Microstructure and wear properties of laser clad carbide coatings. *Int. Congr. Appl. Lasers Electro-Optics* **1993**, 985.
59. Cadenas, M.; Vijande, R.; Montes, H.-J.; Sierra, J.M. Wear behaviour of laser clad and plasma sprayed WC-Co coatings. *Wear* **1997**, *212*, 244–253. [[CrossRef](#)]
60. Ya-Li, G.; Cun-Shan, W.; Man, Y.; Liu, H.-B. The resistance to wear and corrosion of laser-cladding  $\text{Al}_2\text{O}_3$  ceramic coating on Mg alloy. *Appl. Surf. Sci.* **2007**, *253*, 5306–5311.
61. Subramanian, R.; Sircar, S.; Mazumder, J. Laser cladding of zirconium on magnesium for improved corrosion properties. *J. Mater. Sci.* **1991**, *26*, 951–956. [[CrossRef](#)]

62. Ocelík, V.; de Oliveira, U.; de Boer, M.; de Hosson, J.T. Thick Co-based coating on cast iron by side laser cladding: Analysis of processing conditions and coating properties. *Surf. Coat. Technol.* **2006**, *201*, 5875–5883. [\[CrossRef\]](#)
63. De Oliveira, U.; Ocelík, V.; De Hosson, J.T. Analysis of coaxial laser cladding processing conditions. *Surf. Coat. Technol.* **2004**, *197*, 127–136. [\[CrossRef\]](#)
64. Fernández, E.; Cadenas, M.; González, R.; Navas, C.; Fernández, R.; Damborenea, J. de Wear behaviour of laser clad NiCrBSi coating. *Wear* **2005**, *259*, 870–875. [\[CrossRef\]](#)
65. Sun, N.; Shan, H.; Zhou, H.; Chen, D.; Li, X.; Xia, W.; Ren, L. Friction and wear behaviors of compacted graphite iron with different biomimetic units fabricated by laser cladding. *Appl. Surf. Sci.* **2012**, *258*, 7699–7706. [\[CrossRef\]](#)
66. Fernandes, F.; Cavaleiro, A.; Loureiro, A. Oxidation behavior of Ni-based coatings deposited by PTA on gray cast iron. *Surf. Coat. Technol.* **2012**, *207*, 196–203. [\[CrossRef\]](#)
67. Kalpakjian, S.; Schmid, S.R.; Bonacini, M. Plasma Transferred Arc deposition of powdered high performances alloys: process parameters optimisation as a function of alloy and geometrical configuration. *J. Mater. Process. Technol.* **2001**, *37*, 611.
68. Zikin, A.; Ilo, S.; Kulu, P.; Hussainova, I.; Katsich, C.; Badisch, E. Plasma transferred arc (PTA) hardfacing of recycled hardmetal reinforced nickel-matrix surface composites. *Mater. Sci.* **2012**, *18*, 12–17. [\[CrossRef\]](#)
69. Siva, K.; Murugan, N.; Logesh, R. Optimization of weld bead geometry in plasma transferred arc hardfaced austenitic stainless steel plates using genetic algorithm. *Int. J. Adv. Manuf. Technol.* **2009**, *41*, 24–30. [\[CrossRef\]](#)
70. Fernandes, F.; Lopes, B.; Cavaleiro, A.; Ramalho, A.; Loureiro, A. Effect of arc current on microstructure and wear characteristics of a Ni-based coating deposited by PTA on gray cast iron. *Surf. Coat. Technol.* **2011**, *205*, 4094–4106. [\[CrossRef\]](#)
71. Alnaqi, A.A.; Shrestha, S.; Barton, D.C.; Brooks, P.C. *Optimisation of Alumina Coated Lightweight Brake Rotor*; SAE Technical Paper; SAE: Warrendale, PA, USA, 2014.
72. Tong, X.; Li, F.-H.; Liu, M.; Dai, M.-J.; Zhou, H. Thermal fatigue resistance of non-smooth cast iron treated by laser cladding with different self-fluxing alloys. *Opt. Laser Technol.* **2010**, *42*, 1154–1161. [\[CrossRef\]](#)
73. Zhou, H.; Zhang, P.; Sun, N.; Wang, C.-T.; Lin, P.-Y.; Ren, L.-Q. Wear properties of compact graphite cast iron with bionic units processed by deep laser cladding WC. *Appl. Surf. Sci.* **2010**, *256*, 6413–6419. [\[CrossRef\]](#)
74. Fernandes, F.; Polcar, T.; Loureiro, A.; Cavaleiro, A. Effect of the substrate dilution on the room and high temperature tribological behaviour of Ni-based coatings deposited by PTA on grey cast iron. *Surf. Coat. Technol.* **2015**, *281*, 11–19. [\[CrossRef\]](#)
75. Shi, K.; Shubing, H.; Zheng, H. Microstructure and fatigue properties of plasma transferred arc alloying TiC-W-Cr on gray cast iron. *Surf. Coat. Technol.* **2011**, *206*, 1211–1217. [\[CrossRef\]](#)
76. Espallargas, N. *Future Development of Thermal Spray Coatings Types, Designs, Manufacture and Applications*; Elsevier: Cambridge, UK, 2015; ISBN 9781845698126.
77. Herman, H.; Sampath, S. Thermal spray coatings. In *Metallurgical and Ceramic Protective Coatings*; Springer: Dordrecht, the Netherlands, 1996; pp. 261–289.
78. Pawlowski, L. *The Science and Engineering of Thermal Spray Coatings*, 2nd ed.; John Wiley & Sons, Ltd.: Chichester, UK, 2008; ISBN 9780470754085.
79. Tucker, R.C. Thermal spray coatings. *Surf. Eng.* **1993**, *5*, 1446–1471.
80. Sharma, T.K. Performance and emission characteristics of the thermal barrier coated SI engine by adding argon inert gas to intake mixture. *J. Adv. Res.* **2015**, *6*, 819–826. [\[CrossRef\]](#)
81. Gérard, B. Application of thermal spraying in the automobile industry. *Surf. Coat. Technol.* **2006**, *201*, 2028–2031. [\[CrossRef\]](#)
82. Priyan, M.; Hariharan, P.; Shunmuga Priyan, M. Tribology in industry wear and corrosion resistance of Fe based coatings by HVOF sprayed on gray cast-iron for automotive application. *Tribol. Ind.* **2014**, *36*, 394–405.
83. Barbezat, G. Thermal spray coatings for tribological applications in the automotive industry. *Adv. Eng. Mater.* **2006**, *8*, 678–681. [\[CrossRef\]](#)
84. Berger, L.-M.; Puschmann, R.; Spatzier, J.; Matthews, S. Potential of HVOF spray processes. *Therm. Spray Bull.* **2013**, *6*, 16–20.
85. Killinger, A.; Gadow, R.; Mauer, G.; Guignard, A.; Vaen, R.; Stöver, D. Review of new developments in suspension and solution precursor thermal spray processes. *J. Therm. Spray Technol.* **2011**, *20*, 677–695. [\[CrossRef\]](#)

86. Miranda, F.; Caliarì, F.; Essiqtchouk, A.; Pertraconi, G. Atmospheric plasma spray processes: From micro to nanostructures. In *Atmospheric Pressure Plasma—from Diagnostics to Applications*; Caliarì, F., Ed.; IntechOpen: Rijeka, Croatia, 2019; ISBN 978-1-83880-250-9.
87. Tung, S.C.; Mcmillan, M.L. Automotive tribology overview of current advances and challenges for the future. *Tribol. Int.* **2004**, *37*, 517–536. [[CrossRef](#)]
88. Vetter, J.; Barbezat, G.; Crummenauer, J.; Avissar, J. Surface treatment selections for automotive applications. *Surf. Coat. Technol.* **2005**, *200*, 1962–1968. [[CrossRef](#)]
89. Hwang, B.; Lee, S.; Ahn, J. Correlation of microstructure and wear resistance of molybdenum blend coatings fabricated by atmospheric plasma spraying. *Mater. Sci. Eng.* **2004**, *366*, 152–163. [[CrossRef](#)]
90. Skopp, A.; Kelling, N.; Woydt, M.; Berger, L.-M. Thermally sprayed titanium suboxide coatings for piston ring/cylinder liners under mixed lubrication and dry-running conditions. *Wear* **2007**, *262*, 1061–1070. [[CrossRef](#)]
91. Watremez, M.; Bricout, J.P.; Marguet, B.; Oudin, J. Friction, temperature, and wear analysis for ceramic coated brake disks. *J. Tribol.* **1996**, *118*, 457–465. [[CrossRef](#)]
92. Demir, A.; Samur, R. Investigation of the coatings applied onto brake discs on disc-brake pad pair. *Metallurgija* **2009**, *48*, 161–166.
93. Samur, R.; Demir, A. Wear and corrosion performances of new friction materials for automotive industry. *Metallurgija* **2012**, *51*, 94–96.
94. Güney, B.; Mutlu, İ. Tribological properties of brake discs coated  $\text{Cr}_2\text{O}_3$ -40% $\text{TiO}_2$  by plasma spraying. *Surf. Rev. Lett.* **2019**, 1950075. [[CrossRef](#)]
95. Krishnamurthy, N.; Jain, R. Corrosion kinetics of  $\text{Al}_2\text{O}_3 + \text{ZrO}_2 \cdot 5\text{CaO}$  coatings applied on gray cast iron substrate. *Ceram. Int.* **2017**, *43*, 15708–15713.
96. Murthy, J.K.N.; Rao, D.S.; Venkataraman, B. Effect of grinding on the erosion behaviour of a WC-Co-Cr coating deposited by HVOF and detonation gun spray processes. *Wear* **2001**, *249*, 592–600. [[CrossRef](#)]
97. Hawthorne, H.M.; Erickson, L.C.; Ross, D.; Tai, H.; Troczynski, T. The microstructural dependence of wear and indentation behaviour of some plasma-sprayed alumina coatings. *Wear* **1997**, *203–204*, 709–714. [[CrossRef](#)]
98. Hejwowski, T.; Wero, A. The effect of thermal barrier coatings on diesel engine performance. *Vacuum* **2002**, *65*, 427–432. [[CrossRef](#)]
99. Okumus, S.C. Microstructural and mechanical characterization of plasma sprayed  $\text{Al}_2\text{O}_3$ - $\text{TiO}_2$  composite ceramic coating on Mo/cast iron substrates. *Mater. Lett.* **2005**, *59*, 3214–3220. [[CrossRef](#)]
100. Celik, E.; Tekmen, C.; Ozdemir, I.; Cetinel, H.; Karakas, Y.; Okumus, S.C. Effects on performance of  $\text{Cr}_2\text{O}_3$  layers produced on Moyst-iron 2 3 materials. *Surf. Coat. Technol.* **2003**, *174*, 1074–1081. [[CrossRef](#)]
101. Nieminen, R.; Niemi Mantyl, K.T.; Barbezat, G. Rolling contact fatigue failure mechanisms in plasma and HVOF sprayed WC-Co coatings. *Wear* **1997**, *212*, 66–77. [[CrossRef](#)]
102. Ang, A.S.M.; Howse, H.; Wade, S.A.; Berndt, C.C. Development of processing windows for HVOF carbide-based coatings. *J. Therm. Spray Technol.* **2016**, *25*, 28–35. [[CrossRef](#)]
103. Guilemany, J.M. *High Velocity Oxy-Fuel Spraying*; W.S.Maney & Sons Ltd.: Hanover Walk Leeds, UK, 2004; ISBN 1-902653-72-6.
104. Sidhu, T.S.; Prakash, S.; Agrawal, R.D. State of the art of HVOF coating investigations—A review. *Mar. Technol. Soc. J.* **2005**, *39*, 53–64. [[CrossRef](#)]
105. Herman, H.; Sampath, S.; Mccune, R. Thermal spray: Current status and future trends. *MRS Bull.* **2000**, *25*, 17–25. [[CrossRef](#)]
106. Bolelli, G.; Berger, L.M.; Börner, T.; Koivuluoto, H.; Lusvarghi, L.; Lyphout, C.; Markocsan, N.; Matikainen, V.; Nylén, P.; Sassatelli, P.; et al. Tribology of HVOF- and HVOF-sprayed WC-10Co4Cr hardmetal coatings: A comparative assessment. *Surf. Coat. Technol.* **2015**, *265*, 125–144. [[CrossRef](#)]
107. Erning, U.; Nestler, M.C.; Tauchert, G.; Seitz, T.; Prenzel, G. Prenzel HVOF coatings for hard-chrome replacement—Properties and applications. In Proceedings of the DVS Verlag GmbH, UTSC'99: United Thermal Spray Conference, Dusseldorf, Germany, 17–19 March 1999; p. 6.
108. Reignier, C.; Lee, D.; Wet, D.D. HVOF sprayed WC-Co-Cr as a generic coating type for replacement of hard chrome plating. In Proceedings of the International Thermal Spray Conference; ITSC 2002 International Thermal Spray, Essen, Germany, 4–6 March 2002; Volume 2600, pp. 1–8.



109. Matikainen, V.; Bolelli, G.; Koivuluoto, H.; Sassatelli, P.; Lusvarghi, L.; Vuoristo, P. Sliding wear behaviour of HVOF and HVAF sprayed  $\text{Cr}_3\text{C}_2$ -based coatings. *Wear* **2017**, *388–389*, 57–71. [[CrossRef](#)]
110. Bolelli, G.; Berger, L.-M.; Börner, T.; Koivuluoto, H.; Matikainen, V.; Lusvarghi, L.; Lyphout, C.; Markocsan, N.; Nylén, P.; Sassatelli, P.; et al. Sliding and abrasive wear behaviour of HVOF- and HVAF-sprayed  $\text{Cr}_3\text{C}_2$ -NiCr hardmetal coatings. *Wear* **2016**, *358–359*, 32–50. [[CrossRef](#)]
111. Hulka, I.; Şerban, V.A.; Secoşan, I.; Vuoristo, P.; Niemi, K. Wear properties of CrC-37WC-18M coatings deposited by HVOF and HVAF spraying processes. *Surf. Coat. Technol.* **2012**, *210*, 15–20. [[CrossRef](#)]
112. Bolelli, G.; Börner, T.; Milanti, A.; Lusvarghi, L.; Laurila, J.; Koivuluoto, H.; Niemi, K.; Vuoristo, P. Tribological behavior of HVOF- and HVAF-sprayed composite coatings based on Fe-Alloy + WC-12% Co. *Surf. Coat. Technol.* **2014**, *248*, 104–112. [[CrossRef](#)]
113. Bolelli, G.; Bursi, M.; Lusvarghi, L.; Manfredini, T.; Matikainen, V.; Rigon, R.; Sassatelli, P.; Vuoristo, P. Tribology of FeVCrC coatings deposited by HVOF and HVAF thermal spray processes. *Wear* **2018**, *394–395*, 113–133. [[CrossRef](#)]
114. Zimmermann, S. Chromium carbide coatings produced by various HVOF spray system. In *Thermal Spray: Practical Solutions for Engineering Problems*; Berndt, C.C., Ed.; ASM International: Materials Park, OH, USA, 1996; p. 6.
115. Varis, T.; Suhonen, T.; Ghabchi, A.; Valarezo, A.; Sampath, S.; Liu, X.; Hannula, S.-P. Formation mechanisms, structure, and properties of HVOF-sprayed WC-CoCr coatings: An approach toward process maps. *J. Therm. Spray Technol.* **2014**, *23*, 1009–1018. [[CrossRef](#)]
116. Schwetzke, R.; Kreye, H. Microstructure and properties of tungsten carbide coatings sprayed with various high-velocity oxygen fuel spray systems. *J. Therm. Spray Technol.* **1999**, *8*, 433–439. [[CrossRef](#)]
117. Priyan, M.S.; Azad, A.; Araffath, S.Y. Influence of HVOF parameters on the wear resistance of  $\text{Cr}_3\text{C}_2$ -NiCr coating. *J. Mater. Sci. Surf. Eng.* **2016**, *4*, 355–359.
118. Federici, M.; Menapace, C.; Moscatelli, A.; Gialanella, S.; Straffellini, G. Pin-on-disc study of a friction material dry sliding against HVOF coated discs at room temperature and 300 °C. *Tribol. Int.* **2017**, *115*, 89–99. [[CrossRef](#)]
119. Federici, M.; Menapace, C.; Moscatelli, A.; Gialanella, S.; Straffellini, G. Effect of roughness on the wear behavior of HVOF coatings dry sliding against a friction material. *Wear* **2016**, *368–369*, 326–334. [[CrossRef](#)]
120. Öz, A.; Gürbüz, H.; Yakut, A.K.; Sağiroğlu, S. Braking performance and noise in excessive worn brake discs coated with HVOF thermal spray process. *J. Mech. Sci. Technol.* **2017**, *31*, 535–543. [[CrossRef](#)]
121. Wahlström, J.; Lyu, Y.; Matjeka, V.; Söderberg, A. A pin-on-disc tribometer study of disc brake contact pairs with respect to wear and airborne particle emissions. *Wear* **2017**, *384–385*, 124–130. [[CrossRef](#)]
122. Dykhuizen, R.C.; Smith, M.F. Gas dynamic principles of cold spray. *J. Therm. Spray Technol.* **1998**, *7*, 205–212. [[CrossRef](#)]
123. Champagne, V.K. *The Cold Spray Materials Deposition Process*; Woodhead Publishing Limited: Sawston, UK, 2010; ISBN 978-1-84569-181-3.
124. Villafuerte, J. (Ed.) *Modern Cold Spray: Materials, Process, and Applications*; Springer International Publishing: Cham, Switzerland, 2015; ISBN 978-3-319-16771-8.
125. Walker, M. Microstructure and bonding mechanisms in cold spray coatings. *Mater. Sci. Technol.* **2018**, *34*, 2057–2077. [[CrossRef](#)]
126. Singh, H.; Sidhu, T.S.; Kalsi, S.B.S. Cold spray technology: Future of coating deposition processes. *Frat. ed Integrità Strutt.* **2012**, *6*, 69–84. [[CrossRef](#)]
127. Stoltenhoff, T.; Kreye, H.; Richter, H.J. An analysis of the cold spray process and its coatings. *J. Therm. Spray Technol.* **2002**, *11*, 542–550. [[CrossRef](#)]
128. Schmidt, T.; Gaertner, F.; Kreye, H. New developments in cold spray based on higher gas and particle temperatures. *J. Therm. Spray Technol.* **2006**, *15*, 488–494. [[CrossRef](#)]
129. Zhang, D.; Shipway, P.H.; McCartney, D.G. Cold gas dynamic spraying of aluminum: The role of substrate characteristics in deposit formation. *J. Therm. Spray Technol.* **2005**, *14*, 109–116. [[CrossRef](#)]
130. Richer, P.; Yandouzi, M.; Beauvais, L.; Jodoin, B. Oxidation behaviour of CoNiCrAlY bond coats produced by plasma, HVOF and cold gas dynamic spraying. *Surf. Coat. Technol.* **2010**, *204*, 3962–3974. [[CrossRef](#)]
131. Lima, R.; Karthikeyan, J.; Kay, C.; Lindemann, J.; Berndt, C. Microstructural characteristics of cold-sprayed nanostructured WC-Co coatings. *Thin Solid Films* **2002**, *416*, 129–135. [[CrossRef](#)]
132. Poirier, D.; Legoux, J.-G.; Irissou, E.; Gallant, D.; Jiang, J.; Potter, T.; Boileau, J. Performance assessment of protective thermal spray coatings for lightweight al brake rotor disks. *J. Therm. Spray Technol.* **2019**, *28*, 291–304. [[CrossRef](#)]



133. Alhulaifi, A.S.; Buck, G.A.; Arbogast, W.J. Numerical and experimental investigation of cold spray gas dynamic effects for polymer coating. *J. Therm. Spray Technol.* **2012**, *21*, 852–862. [\[CrossRef\]](#)
134. Ogawa, K.; Ito, K.; Ichimura, K.; Ichikawa, Y.; Ohno, S.; Onda, N. Characterization of low-pressure cold-sprayed aluminum coatings. *J. Therm. Spray Technol.* **2008**, *17*, 728–735. [\[CrossRef\]](#)
135. Lioma, D.; Sacks, N.; Botef, I. Cold gas dynamic spraying of WC-Ni cemented carbide coatings. *Int. J. Refract. Met. Hard Mater.* **2015**, *49*, 365–373. [\[CrossRef\]](#)
136. Yandouzi, M.; Sansoucy, E.; Ajdelsztajn, L.; Jodoin, B. WC-based cermet coatings produced by cold gas dynamic and pulsed gas dynamic spraying processes. *Surf. Coat. Technol.* **2007**, *202*, 382–390. [\[CrossRef\]](#)
137. Matikainen, V.; Bolelli, G.; Koivuluoto, H.; Honkanen, M.; Vippola, M.; Lusvarghi, L.; Vuoristo, P. A study of Cr<sub>3</sub>C<sub>2</sub>-based HVOF- and HVAF-sprayed coatings: Microstructure and carbide retention. *J. Therm. Spray Technol.* **2017**, *26*, 1239–1256. [\[CrossRef\]](#)
138. Matikainen, V.; Khanlari, K.; Milanti, A.; Koivuluoto, H.; Vuoristo, P. Spray parameter effect on HVAF sprayed (Fe,Cr)C-30FeNiCrSi hardmetal coatings. In Proceedings of the International Thermal Spray Conference 2016, Shanghai, China, 10–12 May 2016; pp. 184–189.
139. Verstak, A.; Baranovski, V. Deposition of carbides by activated combustion HVAF spraying. In Proceedings of the ITSC 2004: International Thermal Spray Conference 2004: Advances in Technology and Application, Osaka, Japan, 10–12 May 2004; pp. 551–555.
140. Lyphout, C.; Björklund, S.; Karlsson, M.; Runte, M.; Reisel, G.; Boccaccio, P. Screening design of supersonic air fuel processing for hard metal coatings. *J. Therm. Spray Technol.* **2014**, *23*, 1323–1332. [\[CrossRef\]](#)
141. Sadeghimeresht, E.; Reddy, L.; Hussain, T.; Markocsan, N.; Joshi, S. Chlorine-induced high temperature corrosion of HVAF-sprayed Ni-based alumina and chromia forming coatings. *Corros. Sci.* **2018**, *132*, 170–184. [\[CrossRef\]](#)
142. Sadeghimeresht, E.; Markocsan, N.; Nylén, P. Microstructural and electrochemical characterization of Ni-based bi-layer coatings produced by the HVAF process. *Surf. Coat. Technol.* **2016**, *304*, 606–619. [\[CrossRef\]](#)
143. Sadeghimeresht, E.; Markocsan, N.; Nylén, P. Microstructural characteristics and corrosion behavior of HVAF- and HVOF-sprayed Fe-based coatings. *Surf. Coat. Technol.* **2017**, *318*, 365–373. [\[CrossRef\]](#)
144. Lyphout, C.; Björklund, S. Internal diameter HVAF spraying for wear and corrosion applications. *J. Therm. Spray Technol.* **2015**, *24*, 235–243. [\[CrossRef\]](#)
145. Lyphout, C.; Sato, K.; Houdkova, S.; Smazalova, E.; Lusvarghi, L.; Bolelli, G.; Sassatelli, P. Tribological properties of hard metal coatings sprayed by high-velocity air fuel process. *J. Therm. Spray Technol.* **2016**, *25*, 331–345. [\[CrossRef\]](#)
146. Liu, Y.; Liu, W.; Ma, Y.; Meng, S.; Liu, C.; Long, L.; Tang, S. A comparative study on wear and corrosion behaviour of HVOF-and HVAF-sprayed WC-10Co-4Cr coatings. *Surf. Eng.* **2017**, *33*, 63–71. [\[CrossRef\]](#)
147. Wang, Q.; Zhang, S.; Cheng, Y.; Xiang, J.; Zhao, X.; Yang, G. Wear and corrosion performance of WC-10Co4Cr coatings deposited by different HVOF and HVAF spraying processes. *Surf. Coat. Technol.* **2013**, *218*, 127–136. [\[CrossRef\]](#)
148. Toma, F.-L.; Potthoff, A.; Berger, L.-M.; Leyens, C. Demands, potentials, and economic aspects of thermal spraying with suspensions: A critical review. *J. Therm. Spray Technol.* **2015**, *24*, 1143–1152. [\[CrossRef\]](#)
149. Goel, S.; Björklund, S.; Curry, N.; Wiklund, U.; Joshi, S.V. Axial suspension plasma spraying of Al<sub>2</sub>O<sub>3</sub> coatings for superior tribological properties. *Surf. Coat. Technol.* **2017**, *315*, 80–87. [\[CrossRef\]](#)
150. Algenaid, W.; Ganvir, A.; Filomena Calinas, R.; Varghese, J.; Rajulapati, K.; Joshi, S. Influence of microstructure on the erosion behaviour of suspension plasma sprayed thermal barrier coatings. *Surf. Coat. Technol.* **2019**, *375*, 86–99. [\[CrossRef\]](#)
151. Ganvir, A.; Joshi, S.; Markocsan, N.; Vassen, R. Tailoring columnar microstructure of axial suspension plasma sprayed TBCs for superior thermal shock performance. *Mater. Des.* **2018**, *144*, 192–208. [\[CrossRef\]](#)
152. Ganvir, A.; Filomena, R.; Markocsan, N.; Curry, N.; Joshi, S. Experimental visualization of microstructure evolution during suspension plasma spraying of thermal barrier coatings. *J. Eur. Ceram. Soc.* **2019**, *39*, 470–481. [\[CrossRef\]](#)
153. Aranke, O.; Gupta, M.; Markocsan, N. Microstructural evolution and sintering of suspension plasma-sprayed columnar thermal barrier coatings. *J. Therm. Spray Technol.* **2018**, *28*, 198–211. [\[CrossRef\]](#)
154. Tingaud, O.; Bertrand, P.; Bertrand, G. Microstructure and tribological behavior of suspension plasma sprayed Al<sub>2</sub>O<sub>3</sub> and Al<sub>2</sub>O<sub>3</sub>-YSZ composite coatings. *Surf. Coat. Technol.* **2010**, *205*, 1004–1008. [\[CrossRef\]](#)
155. Darut, G.; Ben-Ettouil, F.; Denoirjean, A.; Montavon, G.; Ageorges, H.; Fauchais, P. Dry sliding behavior of sub-micrometer-sized suspension plasma sprayed ceramic oxide coatings. *Proc. Int. Therm. Spray Conf.* **2009**, *19*, 213–218. [\[CrossRef\]](#)

156. Oliker, V.E.; Terent'ev, A.E.; Shvedova, L.K.; Martsenyuk, I.S. Use of aqueous suspensions in plasma spraying of alumina coatings. *Powder Metall. Met. Ceram.* **2009**, *48*, 115–120. [\[CrossRef\]](#)
157. Bannier, E.; Vicent, M.; Rayón, E.; Benavente, R.; Salvador, M.D.; Sánchez, E. Effect of TiO<sub>2</sub> addition on the microstructure and nanomechanical properties of Al<sub>2</sub>O<sub>3</sub> Suspension Plasma Sprayed coatings. *Appl. Surf. Sci.* **2014**, *316*, 141–146. [\[CrossRef\]](#)
158. Darut, G.; Ageorges, H.; Denoirjean, A.; Fauchais, P. Tribological performances of YSZ composite coatings manufactured by suspension plasma spraying. *Surf. Coat. Technol.* **2013**, *217*, 172–180. [\[CrossRef\]](#)
159. Bolelli, G.; Candeli, A.; Lusvarghi, L.; Manfredini, T.; Denoirjean, A.; Valette, S.; Ravaux, A.; Meillot, E. “Hybrid” plasma spraying of NiCrAlY + Al<sub>2</sub>O<sub>3</sub> + h-BN composite coatings for sliding wear applications. *Wear* **2017**, *378–379*, 68–81. [\[CrossRef\]](#)
160. Joshi, S.V.; Sivakumar, G.; Raghuveer, T.; Dusane, R.O. Hybrid plasma-sprayed thermal barrier coatings using powder and solution precursor feedstock. *J. Therm. Spray Technol.* **2014**, *23*, 616–624. [\[CrossRef\]](#)
161. Joshi, S.V.; Sivakumar, G. Hybrid processing with powders and solutions: A novel approach to deposit composite coatings. *J. Therm. Spray Technol.* **2015**, *24*, 1166–1186. [\[CrossRef\]](#)
162. Lohia, A.; Sivakumar, G.; Ramakrishna, M.; Joshi, S.V. Deposition of nanocomposite coatings employing a hybrid APS + SPPS technique. *J. Therm. Spray Technol.* **2014**, *23*, 1054–1064. [\[CrossRef\]](#)
163. Gopal, V.; Goel, S.; Manivasagam, G.; Joshi, S. Performance of hybrid powder-suspension axial plasma sprayed Al<sub>2</sub>O<sub>3</sub>-YSZ coatings in bovine serum solution. *Materials* **2019**, *12*, 1922. [\[CrossRef\]](#)
164. Babu, P.S.; Sen, D.; Jyothirmayi, A.; Krishna, L.R.; Rao, D.S. Influence of microstructure on the wear and corrosion behavior of detonation sprayed Cr<sub>2</sub>O<sub>3</sub>-Al<sub>2</sub>O<sub>3</sub> and plasma sprayed Cr<sub>2</sub>O<sub>3</sub> coatings. *Ceram. Int.* **2018**, *44*, 2351–2357. [\[CrossRef\]](#)
165. Wang, Y.; Jiang, S.; Wang, M.; Wang, S.; Xiao, T.D.; Strutt, P.R. Abrasive wear characteristics of plasma sprayed nanostructured aluminartitania coatings. *Wear* **2000**, *237*, 176–185. [\[CrossRef\]](#)
166. Kiilakoski, J.; Musalek, R.; Lukac, F.; Koivuluoto, H.; Vuoristo, P. Evaluating the toughness of APS and HVOF-sprayed Al<sub>2</sub>O<sub>3</sub>-ZrO<sub>2</sub>-coatings by in-situ-and macroscopic bending. *J. Eur. Ceram. Soc.* **2018**, *38*, 1908–1918. [\[CrossRef\]](#)
167. Bolelli, G.; Cannillo, V.; Lusvarghi, L.; Manfredini, T. Wear behaviour of thermally sprayed ceramic oxide coatings. *Wear* **2006**, *261*, 1298–1315. [\[CrossRef\]](#)
168. Ding, C.; Li, L.; Zhang, X.Y. Wear evaluation of plasma sprayed oxide and carbide coatings. In Proceedings of the Proceedings of the 15th International Thermal Spray Conference, Nice, France, 25–29 May 1998; Volume 1, pp. 25–29.
169. Giroud, A.; Jouanny, C.; Heuze, J.L.; Gaillard, F.; Guiraldenq, P. Friction and corrosion behavior of different ceramic coatings (oxides) obtained by thermal spray for qualification tests in sea water. In *Thermal Spray: Meeting the Challenges of the 21st Century, Proceedings of the 15th International Thermal Spray Conference, Nice, France, 25–29 May 1998*; ASM International: Materials Park, OH, USA; Volume 1, pp. 211–216.
170. Knuuttila, J.; Ahmaniemi, S.; Leivo, E.; Sorsa, P.; Vuoristo, P.; Mantyla, T. Wet abrasion and slurry erosion resistance of sealed oxide coatings. In Proceedings of the 15th International Thermal Spray Conference, Nice, France, 25–29 May 1998; Volume 1, pp. 145–150.
171. Yang, K.; Rong, J.; Liu, C.; Zhao, H.; Tao, S.; Ding, C. Study on erosion-wear behavior and mechanism of plasma-sprayed alumina-based coatings by a novel slurry injection method. *Tribol. Int.* **2015**, *93*, 29–35. [\[CrossRef\]](#)
172. Ouyang, J.H.; Sasaki, S. Effects of different additives on microstructure and high-temperature tribological properties of plasma-sprayed Cr<sub>2</sub>O<sub>3</sub> ceramic coatings. *Wear* **2001**, *249*, 56–66. [\[CrossRef\]](#)
173. Yang, K.; Zhou, X.; Liu, C.; Tao, S.; Ding, C. Sliding wear performance of plasma-sprayed Al<sub>2</sub>O<sub>3</sub>-Cr<sub>2</sub>O<sub>3</sub> composite coatings against graphite under severe conditions. *J. Therm. Spray Technol.* **2013**, *22*, 1154–1162. [\[CrossRef\]](#)
174. Fernlindez, J.E.; Wang, Y.; Tucho, I.; Martin-Luengo, M.A.; Gancedo, R.; Rinc6nt, A. Friction and wear behaviour of plasma-sprayed Cr<sub>2</sub>O<sub>3</sub> coatings against steel in a wide range of sliding velocities and normal loads. *Tribol. Int.* **1996**, *29*, 333–343. [\[CrossRef\]](#)
175. Lyo, I.W.; Ahn, H.S.; Lim, D.S. Microstructure and tribological properties of plasma-sprayed chromium oxide-molybdenum oxide composite coatings. *Surf. Coat. Technol.* **2003**, *163–164*, 413–421. [\[CrossRef\]](#)
176. Yang, X.; Zeng, J.; Zhang, H.; Wang, J.; Sun, J.; Dong, S.; Jiang, J.; Deng, L.; Zhou, X.; Cao, X. Correlation between microstructure, chemical components and tribological properties of plasma-sprayed Cr<sub>2</sub>O<sub>3</sub>-based coatings. *Ceram. Int. J.* **2018**, *44*, 10154–10168. [\[CrossRef\]](#)

177. Ahn, H.-S.; Lyo, I.-W.; Lim, D.-S. Influence of molybdenum composition in chromium oxide-based coatings on their tribological behavior. *Surf. Coat. Technol.* **2000**, *133*, 351–361. [CrossRef]
178. Bagde, P.; Sapate, S.G.; Khatirkar, R.K.; Vashishtha, N.; Tailor, S. Friction and wear behaviour of plasma sprayed Cr<sub>2</sub>O<sub>3</sub>-TiO<sub>2</sub> coating. *Mater. Res. Express* **2018**, *5*. [CrossRef]
179. Yang, K.; Zhou, X.; Zhao, H.; Tao, S. Microstructure and mechanical properties of Al<sub>2</sub>O<sub>3</sub>-Cr<sub>2</sub>O<sub>3</sub> composite coatings produced by atmospheric plasma spraying. *Surf. Coat. Technol.* **2011**, *206*, 1362–1371. [CrossRef]
180. Ahn, H.-S.; Kwon, O.-K. Tribological behaviour of plasma-sprayed chromium oxide coating. *Wear* **1999**, *225–229*, 814–824. [CrossRef]
181. Toma, F.-L.; Potthoff, A.; Barbosa, M. Microstructural characteristics and performances of Cr<sub>2</sub>O<sub>3</sub> and Cr<sub>2</sub>O<sub>3</sub>-15%TiO<sub>2</sub> S-HVOF coatings obtained from water-based suspensions. *J. Therm. Spray Technol.* **2018**, *27*, 344–357. [CrossRef]
182. Cellard, A.; Garnier, V.; Fantozzi, G.; Baret, G.; Fort, P. Wear resistance of chromium oxide nanostructured coatings. *Ceram. Int.* **2009**, *35*, 913–916. [CrossRef]
183. Yang, K.; Feng, J.; Zhou, X.; Tao, S. Microstructural characterization and strengthening-toughening mechanism of plasma-sprayed Al<sub>2</sub>O<sub>3</sub>-Cr<sub>2</sub>O<sub>3</sub> composite coatings. *J. Therm. Spray Technol.* **2012**, *21*, 1011–1024. [CrossRef]
184. Tao, S.; Yin, Z.; Zhou, X.; Ding, C. Sliding wear characteristics of plasma-sprayed Al<sub>2</sub>O<sub>3</sub> and Cr<sub>2</sub>O<sub>3</sub> coatings against copper alloy under severe conditions. *Tribol. Int.* **2009**, *43*, 69–75. [CrossRef]
185. Pantelis, D.I.; Psyllaki, P.; Alexopoulos, N. Tribological behaviour of plasma-sprayed Al<sub>2</sub>O<sub>3</sub> coatings under severe wear conditions. *Wear* **2000**, *237*, 197–204. [CrossRef]
186. Ahn, H.-S.; Kim, J.-Y.; Lim, D.-S. Tribological behaviour of plasma-sprayed zirconia coatings. *Wear* **1997**, *203*, 77–87. [CrossRef]
187. Uyulgan, B.; Cetinel, H.; Ozdemir, I.; Tekmen, C.; Okumus, S.C.; Celik, E. Friction and wear properties of Mo coatings on cast-iron substrates. *Surf. Coat. Technol.* **2003**, *174–175*, 1082–1088. [CrossRef]
188. Mahade, S.; Narayan, K.; Govindarajan, S.; Björklund, S.; Curry, N.; Joshi, S. Exploiting suspension plasma spraying to deposit wear-resistant carbide coatings. *Materials* **2019**, *12*, 2344. [CrossRef]
189. Sahraoui, T.; Fenineche, N.E.; Montavon, G.; Coddet, C. Structure and wear behaviour of HVOF sprayed Cr<sub>3</sub>C<sub>2</sub>-NiCr and WC-Co coatings. *Mater. Des.* **2003**, *24*, 309–313. [CrossRef]
190. Toma, D.; Brandl, W.; Marginean, G. Wear and corrosion behaviour of thermally sprayed cermet coatings. *Surf. Coat. Technol.* **2001**, *138*, 149–158. [CrossRef]
191. Xie, M.; Zhang, S.; Li, M. Comparative investigation on HVOF sprayed carbide-based coatings. *Appl. Surf. Sci.* **2013**, *273*, 799–805. [CrossRef]
192. Mari, D. Cermets and hardmetals BT—Reference module in materials science and materials engineering. In *Reference Module in Materials Science and Materials Engineering*; Elsevier: Amsterdam, the Netherlands, 2016; ISBN 978-0-12-803581-8.
193. Picas, J.A.; Forn, A.; Igartua, A.; Mendoza, G. Mechanical and tribological properties of high velocity oxy-fuel thermal sprayed nanocrystalline CrC NiCr coatings. *Surf. Coat. Technol.* **2003**, *174–175*, 1095–1100. [CrossRef]
194. Li, M.; Shi, D.; Christofides, P.D. Modeling and control of HVOF thermal spray processing of WC-Co coatings. *Powder Technol.* **2005**, *156*, 177–194. [CrossRef]
195. Du, L.; Xu, B.; Dong, S.; Zhang, W.; Zhang, J.; Yang, H.; Wang, H. Sliding wear behavior of the supersonic plasma sprayed WC-Co coating in oil containing sand. *Surf. Coat. Technol.* **2008**, *202*, 3709–3714. [CrossRef]
196. Myalska, H.; Lusvarghi, L.; Bolelli, G.; Sassatelli, P.; Moskal, G. Tribological behavior of WC-Co HVOF-sprayed composite coatings modified by nano-sized TiC addition. *Surf. Coat. Technol.* **2019**, *371*, 401–416. [CrossRef]
197. Crundwell, F.; Moats, M.; Ramachandran, V.; Robinson, T.; Davenport, W.G. *Extractive Metallurgy of Nickel, Cobalt and Platinum Group Metals*; Elsevier: Amsterdam, the Netherlands, 2011; ISBN 9780080968094.
198. Rajasekeran, B.; Theisen, W.; Vassen, R.; Weber, S.; Röttger, A. Mechanical properties of thermally sprayed Fe based coatings. *Mater. Sci. Technol.* **2011**, *27*, 973–982.
199. National Toxicology Program Cobalt-Tungsten Carbide: Powders and Hard Metals. Available online: <http://www.ncbi.nlm.nih.gov/pubmed/21822320> (accessed on 20 March 2019).
200. Suh, M.; Thompson, C.M.; Brorby, G.P.; Mittal, L.; Proctor, D.M. Inhalation cancer risk assessment of cobalt metal. *Regul. Toxicol. Pharmacol.* **2016**, *79*, 74–82. [CrossRef]
201. Milanti, A.; Matikainen, V.; Bolelli, G.; Koivuluoto, H.; Lusvarghi, L.; Vuoristo, P. Microstructure and sliding wear behavior of Fe-based coatings manufactured with HVOF and HVOF thermal spray processes. *J. Therm. Spray Technol.* **2016**, *25*, 1–16. [CrossRef]

202. Sassatelli, P.; Bolelli, G.; Lusvarghi, L.; Manfredini, T.; Rigon, R. Manufacturing and properties of high-velocity oxygen fuel (HVOF)-sprayed FeVCrC coatings. *J. Therm. Spray Technol.* **2016**, *25*, 1302–1321. [[CrossRef](#)]
203. Bolelli, G.; Börner, T.; Bozza, F.; Cannillo, V.; Cirillo, G.; Lusvarghi, L. Cermet coatings with Fe-based matrix as alternative to WC-CoCr: Mechanical and tribological behaviours. *Surf. Coat. Technol.* **2012**, *206*, 4079–4094. [[CrossRef](#)]
204. Bolelli, G.; Hulka, I.; Koivuluoto, H.; Lusvarghi, L.; Milanti, A.; Niemi, K.; Vuoristo, P. Properties of WC-FeCrAl coatings manufactured by different high velocity thermal spray processes. *Surf. Coat. Technol.* **2014**, *247*, 74–89. [[CrossRef](#)]
205. Brezinová, J.; Landová, M.; Guzanová, A.; Dulebová, L.; Draganovská, D. Microstructure, wear behavior and corrosion resistance of WC-FeCrAl and WC-WB-Co coatings. *Metals* **2018**, *8*, 399. [[CrossRef](#)]
206. Berger, L.M.; Hermel, W.; Vuoristo, P.; Mantyla, T.; Lengauer, W.; Ettmayer, P. Structure properties and potentials of WC-Co, Cr<sub>3</sub>C<sub>2</sub>-NiCr and TiC-Ni-based hardmetal like coatings. In *Proceedings of the Thermal Spray: Practical Solutions for Engineering Problems, Proceedings of the 9th National Thermal Spray Conference, Cincinnati, OH, USA, 7–11 October 1996*; ASM International: Materials Park, OH, USA, 1996; pp. 89–96.
207. Stewart, D.; Shipway, P.; McCartney, D. Microstructural evolution in thermally sprayed WC-Co coatings: comparison between nanocomposite and conventional starting powders. *Acta Mater.* **2000**, *48*, 1593–1604. [[CrossRef](#)]
208. Bildstein, M.; Mann, K.; Richter, B. Regenerative braking system. In *Fundamentals of Automotive and Engine Technology*; Reif, K., Ed.; Springer Fachmedien: Wiesbaden, Germany, 2014; pp. 240–243. ISBN 978-3-658-03971-4.
209. Chau, K.T. Pure electric vehicles. In *Alternative Fuels and Advanced Vehicle Technologies for Improved Environmental Performance: Towards Zero Carbon Transportation*; Woodhead Publishing: Sawston, UK, 2014; pp. 655–684. ISBN 9780857095220.
210. Hasegawa, I.; Uchida, S. Railway technology today 7—Braking systems. *Japan Railw. Transp. Rev.* **1999**, *7*, 52–59.
211. Bhandari, P.; Dubey, S.; Kandu, S.; Deshbhratar, R. Regenerative braking systems (RBS). *Int. J. Sci. Eng. Res.* **2017**, *8*, 71–74.
212. Gitlin, J.M. Continental Rethinks the Wheel and the Brake for Electric Cars. Available online: <https://arstechnica.com/cars/2017/08/continental-rethinks-the-wheel-and-the-brake-for-electric-cars/> (accessed on 3 March 2019).



© 2019 by the authors. Licensee MDPI, Basel, Switzerland. This article is an open access article distributed under the terms and conditions of the Creative Commons Attribution (CC BY) license (<http://creativecommons.org/licenses/by/4.0/>).